



1 **DUACS DT2014 : the new multi-mission altimeter dataset**  
2 **reprocessed over 20 years**

3

4 **M.-I. Pujol<sup>1\*</sup>, Y. Faugère<sup>1\*</sup>, G. Taburet<sup>1</sup>, S. Dupuy<sup>1</sup>, C Pelloquin<sup>1</sup>, M. Ablain<sup>1</sup>, N.**  
5 **Picot<sup>2</sup>**

6 [1]{Collecte Localisation Satellites, Toulouse, France}

7 [2]{Centre National Etudes Spatiales, Toulouse, France}

8 [\*]{M.-I. Pujol and Y. Faugere contributed equally to this paper}

9 Correspondence to: M.-I. Pujol (mpujol@cls.fr)

10

11 **Abstract**

12 The new DUACS DT2014 reprocessed products are available since April 2014. Numerous  
13 and impacting evolutions have been implemented at each step of this new data processing.  
14 The main one is the use of a new 20-year altimeter reference period that changes the SLA and  
15 SLA gradient signature. Although all the DUACS products have been improved, this paper  
16 focuses on gridded products quality description over the global ocean. As part as this exercise,  
17 21 years of data have been homogenized allowing us to retrieve accurate large scale climate  
18 signals such as global and regional MSL trend as well as interannual signals, but also refined  
19 mesoscale features.

20 Extensive assessment has been performed on this dataset, which allowed us to establish a  
21 consolidated error budget. The errors at mesoscale are about 1.5cm<sup>2</sup> in low variability areas  
22 and increase to 9cm<sup>2</sup> in average in coastal regions, to reach more than 30cm<sup>2</sup> in high  
23 mesoscale activity areas. The DT2014 products, compared to the previous version DT2010,  
24 presents additional signal for wavelengths lower than ~250km inducing SLA variance and  
25 mean EKE increase of respectively +5.1% and +15%. Comparison with independent  
26 measurements underlined the improved mesoscales restitution with this new dataset. The  
27 errors reduction at mesoscale reaches nearly 10% of the error observed with DT2010. The  
28 DT2014 also presents improved coastal signal with a 2 to 4% mean error reduction. High  
29 latitudes areas are also better represented in DT2014, with a better consistency between map



1 spatial coverage and sea ice edge position. The budget error is finally discussed, in order to  
2 highlight the limitation of gridded products, notably in strong internal tide area.

3

#### 4 **1 Introduction**

5 Since its beginning in late 1997, the DUACS (Data Unification and Altimeter Combination  
6 System) system aims at producing and delivering high quality along track (L3 products) and  
7 multi-mission gridded (L4 products) altimeter products directly usable by a large variety of  
8 users and for different applications. They are delivered both in Near Real Time (NRT), with a  
9 delay comprised between few hours to one day, and completely reprocessed about every three  
10 years thanks to a Delayed Time (DT) mode. During the last two decades, successive papers  
11 have described the evolution of the DUACS system and its associated products (Le Traon et  
12 al, 1992; 1995; 1999; 2003; Ducet et al, 2000; Pujol et al, 2005; Dibarboure et al., 2011). In  
13 overall, the products quality is impacted by several factors as the altimetry constellation used  
14 in input (Pascual et al, 2006; Dibarboure et al, 2011), the choice of the altimeters standards  
15 (Dibarboure et al, 2011; Ablain et al, 2015) and the improvement of the data processing  
16 algorithm (Ducet et al, 2000; Dussurget et al, 2011; Griffin et al, 2012; Escudier et al, 2013) .

17 This paper is dedicated to the new global reprocessing that covers the entire altimeter period  
18 and allows us for the first time to generate a gridded product time series of more than 20  
19 years, identified as DT2014. The period starts at the beginning of the altimeter era and ranges  
20 from 1993 to 2013. Measurements from 10 altimeters missions (repetitive and geodetic orbits)  
21 have been used : the TOPEX/Poseidon (TP) and Jason series (Jason-1 (J1) & Jason-2 (J2)),  
22 ERS-1/2 and ENVISAT (EN), Geosat Follow On (GFO), Cryosat-2 (C2), AltiKa (AL) and  
23 Haiyang-2A (HY-2A). It upgrades the previous version (called DT2010; Dibarboure et al.,  
24 2011) and still pursues the same objectives that first consist in generating time series as  
25 homogeneous and up to date as possible and in providing in a gridded product containing a  
26 large panel of ocean signals from the mesoscales to the ocean climate scales. To achieve this  
27 objective, various algorithms and corrections developed in the research community and  
28 through different projects and programs as the French SALP/AVISO, the European  
29 Myocean2 and European Space Agency (ESA) Climate Change Initiative projects. The  
30 development of regional experimental DUACS products in the framework of scientific  
31 oceanographic campaign such as KEOPS-2 (d'Ovidio et al, 2015) was also valuable to assess  
32 locally the improvement, before the implementation in the global product. However, one of



1 the main priorities was to improve the monitoring of the mesoscales in the global ocean.  
2 Indeed, recent papers (Dussurget et al, 2011, Chelton et al, 2011, Escudier et al. 2013) have  
3 shown that despite the accuracy of the DT2010 gridded products, the mesoscale signals  
4 interpolation are limited by the anisotropy of the altimetry observing system, and finer scale  
5 signals contained in the altimeter raw measurements are not really exploited and provided in  
6 the higher level DUACS products (L3 and L4). In addition to these mesoscales retrieval  
7 improvements and to satisfy the large panel the AVISO's users, the new DT2014 reprocessing  
8 product also benefited from climate standards and corrections that do not degrade the  
9 mesoscale signals. Thus, the different choices and trade-off decided to generate the DT2014  
10 reprocessing are described in details in this paper.

11 The DT2014 reprocessing is characterized by important changes in terms of altimeter  
12 standards, data processing and format. The main changes consist in referencing the SLA  
13 products on a new altimeter reference period, taking advantage of the 20 years of  
14 measurements available; optimizing the along-track random noise reduction when in the  
15 DT2010 version a large part of the physical signal was impacted by this processing. It results  
16 important impact in the physical content of the SLA and derivated products. The gridded  
17 products are constructed using more accurate parameters (e.g. correlation scales, error  
18 budgets) and directly on the  $1/4^\circ \times 1/4^\circ$  Cartesian grid resolution. Other changes implemented  
19 allowed us to correct different anomalies detected on the previous DT2010 products. The  
20 resulting quality sea surface and current products is improved. We present in this paper this  
21 last version of the DT2014 products and its improvements compared to the previous version.

22 The paper is organized as follows: the altimeter L3/L4 data processing, with changes  
23 implemented in the DT2014 products, is presented in section 2. Then, in section 3, the results  
24 obtained with the DT2014 reprocessed products are compared to the DT2010 results focusing  
25 on mesoscales and coastal areas. In the same section, we give for the first time an estimation  
26 of the L4 product errors. Finally, a summary of the key results obtained are given in section 4.

27

## 28 **2 Data Processing**

### 29 **2.1 Altimeter standards**

30 The altimeter standards used in DT2014 were selected taking advantage of the work  
31 performed in the first phase of the Sea Level Climate Change Initiative (SL\_cci) led by the



1 ESA in 2011-2013. This project aimed to generate the optimal reprocessed products for  
2 climate application, notably global and regional mean sea level trend. As part of this exercise,  
3 a rigorous selection process was set in place. This process, as well as all the standards  
4 selected, is described in Ablain et al, 2015. As recommended by the SL\_cci project, two  
5 major standards were changed in the DT2014 products, compared to the DT2010. First, new  
6 orbit solutions were used: GDR-D (or equivalent) standards for Envisat, Jason-1, Jason-2 and  
7 Cryosat, and REAPER solution (Rudenko et al, 2012) for ERS-1 and ERS-2. Then, the ERA  
8 Interim reanalyzed atmospheric fields were used in the Dynamic Atmospheric Correction and  
9 dry troposphere corrections.

10 In the Aviso/Myocean-2 context, we also needs to insure an optimal restitution of the  
11 mesoscale signal, some adjustments in the standards selection were done. Notably, whereas  
12 the ERA Interim based corrections are considered over the whole altimeter period in the  
13 SL\_cci project, we used it only during the first decade (i.e. for TP, ERS-1/2) in the DUACS  
14 products. Indeed, evaluations done within SL\_cci project (Carrere et al. (2015); Ablain et al,  
15 2015) clearly underlined that the use of ERA-Interim based correction (instead of ECMWF  
16 operational fields) strongly improves mesoscales and regional spatial scales observation for  
17 the first altimetry decade, while not significant improvement is observed from 2004.

18 The details of the altimeter standards used in the DT2014 products are given in AVISO  
19 (2014b).

## 20 **2.2 DUACS DT2014 processing**

### 21 **2.2.1 Overview of the DUACS DT processing**

22 The DUACS DT processing includes different steps as described by Dibarboure et al (2011).  
23 They consist in acquisition, homogenization, input data quality control, multi-missions cross-  
24 calibration, along-track SLA generation, multi-missions mapping, final quality control and  
25 finally dissemination of the products. From the along-track and gridded SLA products thus  
26 obtained, different derivated products as geostrophic velocities are also computed. We  
27 summarizes here the changes in the different processing steps of the DUACS DT system that  
28 have direct impacts on the products accuracy and for the users.

29 Acquisition/homogenization:



1 60+ cumulative years of different datasets were acquired over the 21-year period [1993,  
2 2013]. They include measurements from the 10 different altimeters ERS-1/2, EN (repetitive  
3 and geodetic orbits), TP, J1 (repetitive, tandem and geodetic end of life orbit), J2, GFO, C2,  
4 AL and HY-2A. The different period covered by the different altimeters is summarized in Fig.  
5 1. The main differences with DT2010 is the introduction of the year 2011 for C2 and the first  
6 cycles of J1 geodetic orbit (cycle 500 to 505, May to mid June 2012).

7 *Input data quality control:*

8 The detection of invalid measurements was based on the approach set up for DT2010 and was  
9 improved, on one hand, for non repetitive orbit missions (J1 geodetic, C2) that are more and  
10 more present in the reprocessing, and in the other hand, in new areas as the coastal zone (all  
11 the missions) and high latitudes (C2, AL). As these new missions are able to sample the ocean  
12 surface in areas never reached by other altimeters, they are usually contaminated by the  
13 reduced quality of geophysical corrections and Mean Sea Surface in these specific areas. Such  
14 anomalies were observed in the DT2010 products and introduced anomalies on gridded  
15 products. In order to avoid this problem in the DT2014 products, the criteria used for the  
16 detection of erroneous measurements was strongly restricted in coastal areas. The  
17 measurements along non repetitive orbits are rejected when closer to the coast than 20 km. In  
18 the same way, the bad quality of the Mean Sea Surface (MSS) in the Laptev Sea conduces to  
19 the systematic detection of the measurements along non repetitive orbits in this area. The use  
20 of a MSS to generate SLA along non repetitive orbits is discussed in “Along-track SLA  
21 generation” paragraph

22 *Multi-mission homogenization and cross-calibration:*

23 The first homogenization step, consists in acquiring the altimeter and ancillary data as  
24 homogeneous as possible for the different altimeters. They include the most recent standards  
25 recommended for altimeter products by the different agencies and expert groups as OSTST,  
26 ESA Quality Working groups or ESA SL\_cci project. The up to date standards used for  
27 DT2014 are described and discussed in the Sect. 2.1.

28 Although the raw input L2 GDR datasets are properly homogenized and edited (see “*Input*  
29 *data quality control*”), they are not always coherent due to various sources of geographically  
30 correlated errors (instrumental, processing, orbits residuals errors). Consequently, the multi-  
31 mission cross-calibration aims at reducing the errors in order to generate a global, consistent  
32 and accurate data set for all altimeters constellation.



1 The second homogenization step, crucial for climate signal, consists in ensuring the mean sea  
2 level continuity between the three altimeter reference missions. The DUACS DT system uses  
3 first TP from 1993 to April 2002, then J1 until October 2008 and finally J2 that covers the end  
4 of the period. This processing step consists in reducing the global and regional biases for each  
5 transition (T/P-J1 and J1-J2) using the calibration phase of the J1 and J2 altimeters where  
6 altimeters are on the same orbit, with few hours of phase offset. Thus, a first polynomial  
7 adjustment allows to reduce the latitude dependant biases between the two successive  
8 reference missions as well as the global mean bias observed between the two successive  
9 missions. A second adjustment consists in reducing the regional long wavelength residual  
10 biases. As illustrated on Fig. 2 it permits to remove large spatial pattern (basin scale) errors of  
11 the order of 1-2 cm.

12 Then, a cross-calibration process consists in reducing the orbit errors by a global  
13 minimization of the crossover differences observed for the reference mission and between  
14 reference and secondary missions. No specific change was implemented for this step of the  
15 processing in the reprocessed version.

16 The last step consists to apply the long wavelength errors (LWE) reduction algorithm. This  
17 process reduces the geographically correlated errors between neighboring tracks from  
18 different sensors. This empirical correction based on optimal interpolation (Le Traon et al.  
19 1998, Ducet et al., 2000) also contributes to reduce the residual high frequency signal that is  
20 not fully corrected with the different corrections applied (mainly Dynamic Atmospheric  
21 Correction and Ocean tides). This empirical processing need an accurate description of the  
22 variability of the error signal associated to the different altimeter missions. In the DT2014  
23 products, the long-wavelength residual ionosphere signal, that can be observed when this  
24 correction is deduced from a model (typically for mission with mono-frequency  
25 measurement), is taken into account for ERS-2, C2 and HY-2A. In the same way, geodetic  
26 missions, for which no precise mean profile is available (see hereafter), present additional  
27 long-wavelength errors induced by the use of a global gridded Mean Sea Surface for SLA  
28 computation. These MSS additional errors were taken into account in the reprocessed  
29 products for C2, J1 geodetic phase, EN on it geodetic orbit and HY-2A.

### 30 Along-track SLA generation:

31 In order to take advantage of the repetitive characteristics of some altimeter missions and to  
32 ease the use of altimeter products by the users, the measurements are co-located on theoretical



1 positions, allowing us to estimate a precise Mean Sea Surface (MSS) along these tracks, also  
2 named Mean Profile (MP). The MPs are time average of the co-located Sea Surface Height  
3 (SSH) measured by the altimeters. The DT2014 reprocessing includes the reprocessing of  
4 these MPs along the TP/J1/J2, TP-tandem/J1-tandem, ERS-1/ERS-2/EN and GFO tracks.  
5 Indeed, they need to be consistent with the altimeter standards used (see Sect. 2.1), and the  
6 MSS also used for non repetitive missions (see here after). The MP reprocessing included  
7 specific efforts to improve the accuracy and extend their estimation in the high latitudes areas.  
8 One of the main changes included in this MPs reprocessing is the use of a new 20-year [1993,  
9 2012] altimeter reference period, as better explained in Sect. 2.2.2. Additionally, the precision  
10 of the different MPs was improved combining the altimeter data that are on the same orbit. In  
11 this way, TP, J1 and J2 measurements are all used to define the corresponding MP; TP  
12 tandem and J1 tandem or ERS-2 and EN are also merged. This processing leads to an  
13 improved definition of the MPs near the coast, with in particular a gain of defined positions  
14 near from the coast. The number of points defined within 0-15km far from the coast in the  
15 newest MPs is indeed twice (tree time) the number observed in the previous version of the  
16 MPs, respectively along TP and TPN theoretical tracks. In the same way, additional 15 to  
17 20% points are defined near the coast, along G2 and EN theoretical tracks in the newest MPs.  
18 The MP along EN theoretical tracks is also better defined in the high latitudes areas, taking  
19 advantage of the more important ice melt occurring after year 2007 (Fig. 3).

20 In the case of the non repetitive missions (i.e. ERS-1 during the geodetic phase; EN after the  
21 orbit change; J1 on the geodetic phase; C2), or recent mission following a newest theoretical  
22 track (i.e. HY-2A), the estimation of a precise MP is not possible. In that case, the SLA is  
23 estimated along the real altimeter tracks, using a gridded MSS as reference. The later is the  
24 MSS\_CNES\_CLS\_11 described by Schaeffer et al (2012), and corrected in order to be  
25 representative of the 20-year [1993, 2012] period (see also Sect. 2.2.2).

26 The SLA, obtained by subtracting the MP or MSS on the SSH measured by the  
27 altimeter, is affected by measurement noises. A Lanczos low pass along-track filtering allows  
28 us to reduce this noise. Two different filtering parameterizations are used, according to the  
29 application. For the generation of the L3 along-track products, the cut-off wavelength was  
30 revisited in the DT2014 in order to reduce as much as possible the random measurement  
31 noise, keeping safe the dynamic signal. More details are given in Sect. 2.2.3. The along-track  
32 measurements are also filtered in view of the mapping process. In this case, the filtering also



1 aims to reduce the signature of the short scales signal that cannot be properly mapped (mainly  
2 due to limitation of altimetry spatial and temporal sampling). The wavelengths ranging nearly  
3 200 to 65 km are filtered (latitude dependant). Finally, the along-track measurements are sub-  
4 sampled in order to keep one point over two, leading to a nearly 14km distance between two  
5 successive points. Because some applications need the full resolution data, the non-filtered  
6 and non-sub-sampled products are also distributed in DT mode.

7 *Multi-mission mapping:*

8         The mapping procedure aims to construct a regularly gridded SLA field combining  
9 measurements from different altimeters. The DUACS mapping processing mainly focus on  
10 mesoscale signal reconstruction. It uses an Optimal Interpolation (OI) processing as described  
11 in Ducet et al (2000) and Le Traon et al (2003). This methodology needs a description of the  
12 characteristics of the physical signal we want to map. The parameters used for the mapping  
13 procedure are a compromise between the characteristics of the physical field we focus on, and  
14 the altimeter constellation sampling capabilities. The parameters used in the DT2014 OI  
15 processing were refined.

16 The main improvements consist in computing the maps with a daily sampling (i.e. a map is  
17 computed for each days of the week, while only map centered on Wednesday was computed  
18 in DT2010). A second important change is the definition of the grid points with a global  
19 Cartesian  $1/4^\circ \times 1/4^\circ$  resolution. This choice was mainly driven by user requests since  
20 Cartesian grids manipulation is simplest compared to a Mercator projection. Compared to the  
21 historical  $1/3^\circ \times 1/3^\circ$  Mercator resolution, the Cartesian projection leads to an improved  
22 resolution between latitude of nearly  $\pm 41.5^\circ\text{N}$ , as illustrated in (Fig. 4). These latitudes  
23 include the main part of the high variability mesoscales areas, like the Gulf Stream, Kuroshio,  
24 Agulhas current and North of the confluence area. Up to these latitudes, the meridian  
25 resolution is reduced in the Cartesian projection, reducing the capability of the gridded  
26 products to accurately represents the mesoscale signal in high latitudes areas. Additionally to  
27 the grid standards change, the area defined by the global product was extended up to the poles  
28 in order to take into account the high latitude sampling offered by the recent altimeters like  
29 C2 (i.e. up to  $\pm 88^\circ\text{N}$ ).

30 Another important change implemented in DT2014 is the use of better defined correlation  
31 scales of the signal we want to map, and a more precise estimation of the errors budget  
32 associated with the different altimeter measurements. These two parameters indeed have a





1 direct impact for mapping improvement as underlined by previous studies (Fieguth et al,  
2 1998; Ducet et al 2000; Leben et al 2002; Griffin et al, 2012, among others). The spatial  
3 variability of the spatial and temporal scales of the signal (see Dibarboure et al, 2011) is better  
4 taken into account. The additional errors induced by the geodetic characteristics of some  
5 orbits (and so the use of a gridded MSS rather than a more precise MP, as explained here  
6 before) are taken into account. In the same way, we also included additional errors for the  
7 altimeters for which the absence of dual-frequency and/or radiometer measurements lead to  
8 the necessity to use model correction for ionospheric and dry-troposphere signal corrections.

9 As previously, two gridded products are computed, using two different altimeter  
10 constellations. The all-sat-merged products take advantage of all the altimeter measurements  
11 available. This allows an improved signal sampling when more than 2 altimeters are available  
12 (Fig. 1). The mesoscale signal is indeed better reconstructed during these periods (Pascual and  
13 al, 2006), when omission errors are reduced by the altimeter sampling. In the same way, high  
14 latitudes areas can be better sampled by one of the altimeters available. These products are  
15 however not homogeneous in time, leading to interannual variability of the signal directly  
16 linked with the evolution of the altimeter sampling. In order to avoid this phenomenon, the  
17 two-sat-merged products are also delivered. They merge two altimeters following the TP and  
18 ERS-2 tracks (e.g. TP, then J1 then J2 merged with ERS-1 then ERS-2 then EN then AL (or  
19 C2 when neither EN nor AL are available)) in order to secure as much as possible the  
20 temporal homogeneity of the products. Except the difference of altimeter constellation, the  
21 mapping parameters are the same for the all-sat-merged and two-sat-merged products.

#### 22 Products format and nomenclature:

23 The DT2014 products are distributed in a NetCDF-3CF format convention and with a new  
24 nomenclature for files and directories names. Details are given in the user handbook  
25 (AVISO/DUACS, 2014b).

#### 26 2.2.2 Reference period and SLA reference convention

27 Due to the poor knowledge of the Geoid at small scales and to ease the use of the altimeter  
28 DUACS products, the altimeter measurements are co-located on theoretical track and a time  
29 average is removed (Dibarbouré et al 2011). Consequently, the sea level anomalies provided  
30 in the L3 and L4 DUACS products are representative of variations of the sea level relative to  
31 the given period, called the altimeter reference period. Since 2001, they have been referenced



1 to a 7-year period [1993, 1999]. In 2014, with more than 20 years of altimeter measurements  
2 available, it was of high interest to extend the altimeter reference period to 20 years [1993-  
3 2012].

4 Changing from a 7 to 20 years reference period leads to obtain more realistic oceanic  
5 anomalies, in particular the interannual and climate scales. Indeed, The change of reference  
6 period from 7 years to 20 years integrates the evolution of the sea level in terms of trends, but  
7 also in terms of interannual signals at small and large scales (e.g. Niño/Niña) in the 13 last  
8 years. Fig. 6 (b) shows an example of this impact on a specific track of J2 over the Kuroshio  
9 region. It clearly underlines a different SLA signature of the amplitude of the stream. The  
10 reference period change from 7 years to 20 years, induces the global and regional Mean Sea  
11 Level (MSL) variations, and is plotted in Fig. 6 (a). It represents the change that users observe  
12 in the DT2014 version of the product compared to DT2010. It also includes the adjustment of  
13 the SLA bias convention. It consists of having a mean SLA null over the year 1993. The use  
14 of this convention for the SLA leads to the introduction of a SLA bias between the DT2014  
15 products and the former version. In Delayed time, this bias is estimated at nearly 0.6 cm.

16 The altimeter reference period change also impacts the Mean Dynamic Topography (MDT)  
17 field. Indeed, as long as the MDT is combined with SLA in order to estimate the Absolute  
18 Dynamic Topography (ADT), the reference period the MDT refers to must be coherent with  
19 the reference period the SLA refers to. The last MDT\_CNES\_CLS13 (Rio et al, 2010)  
20 available on AVISO is distributed on a 20-year reference period, consistent with SLA  
21 DT2014 products.

22 The Annex gives an overview of the relation between SLA and MDT over different reference  
23 periods.

### 24 2.2.3 L3 Along-track noise filtering

25 As explained in the Sect. 2.2.1, the gridded products processing parameters is a trade-off  
26 between the altimeter constellation sampling capability and signal to retrieve. For DT2010,  
27 the processing, and in particular the along track noise filtering was set up in accordance to this  
28 objective. Consequently, the global DT2010 along-track SLA products were so far low-pass  
29 filtered with lanczos cut-off lengths depending on latitude (250km near Equator, until 55km at  
30 high latitudes). This technical choice was mostly linked to the ability of the TP altimeter  
31 mission to capture ocean dynamics mesoscale structures (Le Traon and Dibarboure 1999).



1 However it reduced strongly the along-track resolution that might be useful and beneficial to  
2 modeling and forecasting systems. That is why a dedicated along track product, preserving  
3 the along track 1Hz high resolution signals has been developed in the frame of the DT2014  
4 reprocessing. The main inputs come from the Dufau et al study (2014).

5 This study is based on spectral analysis, where the minimum length scale reachable with  
6 along-track altimeter data is determined as the point where signal and error are of the same  
7 order of magnitude. The mesoscale capability average over the World Ocean is 55km but  
8 appears lower in the equatorial band (20°S-20°N) and in the Western Boundaries Currents.  
9 The small-scale capability prescribed by this method at low latitudes being partly due to the  
10 limit of the underlying Surface Quasi-Geostrophy turbulence in these areas, this region is  
11 retrieved. The mean mesoscale capability used as the cut-off length for low-pass filtering is  
12 consequently 65km.

### 13 **2.3 DT2014 gridded products validation protocol**

14 The comparison between the DT2014 and DT2010 products, as well as the comparison  
15 between altimeter gridded products and independent measurements, are presented in section  
16 3. We discuss in the section the methodology on comparison of the different products.

#### 17 **2.3.1 Altimeter gridded products intercomparison**

18 DT2014 and DT2010 SLA gridded products were compared over they common period [1993,  
19 2012]. The DT2010 products were first processed in order to homogenize the resolution and  
20 physical content. In this way,

- 21 – The DT2010 products considered correspond to the  $\frac{1}{4}^{\circ} \times \frac{1}{4}^{\circ}$  Cartesian resolution  
22 products previously identified as “QD” products. These products were deduced from  
23 the DT2010 original grid resolution ( $\frac{1}{3}^{\circ} \times \frac{1}{3}^{\circ}$  Mercator grid, see Sect. 2.2.1) by bi-  
24 linear interpolation..
- 25 – The DT2010 SLA was referenced to the 20-year altimeter reference period (see Sect.  
26 2.2.2). The reader must note that this reference change is not applied when working on  
27 ADT field since ADT is not impacted by altimeter reference period as explained in  
28 Annex.



1 The geostrophic currents and derived EKE were also compared. In this order, geostrophic  
2 currents were computed using the same methodology (here centered differences) both on  
3 DT2010 and DT2014 products.

#### 4 2.3.2 Comparison between gridded products and independent along-track 5 measurements

6 The gridded products quality is estimated by comparing SLA maps with independent along-  
7 track measurements. Maps merging only two altimeters (i.e. “two-sat-merged” products; see  
8 Sect. 2.2.1) are compared with SLA measured along the tracks following other orbits. This is  
9 possible only when three or four altimeters are available. In this way, TP tandem (TPN) is  
10 compared with gridded product over the years 2003-2004. The SLA is filtered in order to  
11 compare wavelength ranging 65-500km, characterizing medium and large mesoscale signals.  
12 The smallest scale (less than 65km) are excluded in order to reduce the impact of along-track  
13 random errors (see Sect. 2.2.3). The variance of the SLA differences between gridded product  
14 and along-track measurements is analyzed over different spatial selections. The same  
15 comparison is done using the previous DT2010 version of the products (processed as  
16 described in section 2.3.1) in order to estimate the improved accuracy of the new DT2014  
17 products. We assume as a first approximation that the errors observed on along-track products  
18 at these wavelength is lower than the errors of the gridded products. Indeed, mapping  
19 processing lead to the smoothing/missing of the small scales signal, as previously discussed,  
20 and random noise signal observed on along-track products is minimized by the filtering  
21 applied. The variance of the differences between grids and along-track thus mainly traduces  
22 the imprecision of mesoscales reconstruction with gridded products. This is however a strong  
23 approximation since it did not consider correlated errors between both the datasets (the  
24 altimeter standards used are quite homogeneous from an altimeter to the other).

#### 25 2.3.3 Comparison between gridded products and in-situ measurements

26 Different in-situ measurements were used during the validation of the altimeter gridded  
27 products. We present in this section the methodology used for the different in-situ  
28 comparisons.

29 Tide gauges:



1 Monthly mean Tide Gauges (TGs) from PSMSL (Permanent Service for Mean Sea Level)  
2 database with a long life time (> 4 years) were used. The TG data processing is described by  
3 Valladeau et al (2012) and Prandi et al. (2015). The Sea Surface Height measured by the TGs  
4 is compared to the monthly mean SLA field given by altimeter gridded products merging all  
5 the altimeters available (i.e. “all-sat-merged” products). As described by Valladeau et al  
6 (2012) and Prandi et al. (2015), data collocation is based on a maximal correlation criterion.

#### 7 Temperature/Salinity profiles:

8 Quality controlled Temperature/Salinity (T/S) profiles from Coriolis Global Data Assembly  
9 Center were used. The T/S profiles processing used in this paper is the same as described by  
10 Valladeau et al (2012) and Legeais et al (2015). The Dynamic Height Anomalies (DHA)  
11 deduced from T/S profiles are then compared to the equivalent field deduced from gridded  
12 “all-sat-merged” SLA products.

#### 13 Surface drifters:

14 Surface drifters distributed by AOML (Atlantic Oceanographic & Meteorological Laboratory)  
15 over the 1993-2011 were processed in order to extract the absolute geostrophic component  
16 only. In this way, they were corrected from Ekman component using the model described by  
17 Rio et al (2011). Drifters’ drogue loss was detected and corrected using the methodology  
18 described by Rio et al., (2012). A low-pass 3-day filtering is applied in order to reduce the  
19 inertial wave effect. Finally, the absolute geostrophic current deduced from altimeter “all-sat-  
20 merged” maps are interpolated on drifters positions for comparison.

21

### 22 **3 DT2014 products analysis**

#### 23 **3.1 Mesoscale signal in along-track products**

24 The unique cut-off length of 65km used for along-track products filtering (see Sect. 2.2.3)  
25 drastically changes the content of SLA profiles especially in low latitudes areas where  
26 wavelengths from nearly 250km (near the equator) to 120 km (near  $\pm 30^\circ\text{N}$ ) were filtered in  
27 the DT2010 products. Higher resolution SLA profiles are now provided.

28 Spectral analysis applied on new products confirms that addition of energy in the mesoscale  
29 dynamics band at low latitudes: The new SLA preserve the energy of unfiltered data until a  
30 length scale of 80km in the equatorial band, but also in the mid latitudes high variability areas



1 though less impacted by this filtering change. Fig. 5 shows the variance of the short  
2 wavelength signal filtered from J2 along-track products over year 2012, both in DT2010 and  
3 DT2014 versions. The figure underlines an important variance in the middle latitudes areas  
4 and equatorial region. It is directly linked to the 1Hz altimeter measurement error highly  
5 correlated with the significant wave height and unhomogeneity in the radar backscatter  
6 coefficient (Dibarboure et al, 20114; Dufau et al, 2014, in review). In the DT2010 dataset, the  
7 wavelength signal filtered is clearly more important in the latitudes ranging  $\pm 40^{\circ}\text{N}$ ,  
8 underlining part of the physical signal.

### 9 **3.2 Mesoscale signal in gridded products**

#### 10 **3.2.1 Additional signal observed in DT2014 compared to DT2010**

11 The mapping process optimization (see Sect. 2.2.1) directly impacts the SLA physical  
12 content observed with gridded products. The differences between DT2014 and DT2010  
13 temporal variability of the signal for the period [1993, 2012] is shown in Fig. 7 (“all-sat-  
14 merged” product). It underlines additional variability in the DT2014 products. The global  
15 mean SLA variance is now increased by nearly  $+3.5\text{ cm}^2$  within the latitudes band  $\pm 60^{\circ}\text{N}$ . It  
16 represents 5.1% of the variance of the DT2010 products. This increase is mainly due to the  
17 mapping parameters including two main changes in the DT2014 products. The first one, that  
18 explains +3.6% of the variance increase, is the change of the grid resolution. Indeed, the  
19 DT2014 was directly computed on the  $1/4^{\circ}\times 1/4^{\circ}$  Cartesian grid resolution (see Sect. 2.2.1),  
20 while the DT2010 “QD” product considered was not directly computed on this grid resolution  
21 but is deduced from the original  $1/3^{\circ}\times 1/3^{\circ}$  Mercator resolution product by linear interpolation  
22 (see Sect. 2.3.1). This processing slightly smoothes the signal, and directly contributes to  
23 reduce the variance of the signal observed in DT2010. The second change implemented in the  
24 DT2014 products is the use of improved correlation scales. It contributes to increase the SLA  
25 variance by +1.5%. Finally, additional measurements (e.g. C2 in 2011) that were not included  
26 in the DT2010 products also contribute to improve the signal sampling, and thus increase the  
27 variance of the gridded signal.

28 The additional signal observed in the DT2014 products is not uniformly distributed as  
29 underlined in Fig. 7. Indeed, the main part of the variance increase (from +50 to more than  
30  $+100\text{ cm}^2$ ) is observed in the higher variability areas and coastal areas. It traduces the better  
31 reconstruction of the mesoscale signal in the DT2014 products, as discussed after. In some



1 part of the Ocean we however observe a decreasing of the SLA variance. The improved  
2 standards used (see Sect. 2.1) indeed contribute to locally reduce the SLA error variance. The  
3 main reduction is observed in the Indonesian area with an amplitude ranging 2 to 3  $\text{cm}^2$ . The  
4 SLA error variance is also reduced in the Antarctic area (latitudes  $< 60^\circ$ ) with the locally  
5 higher amplitude. The improved DAC correction using ERA-Interim fields over the first  
6 decade of the altimeter period, largely contributes to the variance reduction (Carrere et al.,  
7 2015).

8 The analysis of the spectral content of the gridded products over the Gulf Stream area (Fig. 9)  
9 shows that all DT2014 products are impacted at small scales, i.e. wavelength lower than 250-  
10 200 km. For “all-sat-merged” as well as “two-sat-merged” the energy for wavelength around  
11 100km are twice more important in the DT2014 than in the DT2010 maps, both in zonal and  
12 meridian directions. The maximum additional signal is observed for wavelength ranging 80-  
13 100 km. For these wavelengths the DT2014 products have 2 to 4 times more energy than in  
14 the DT2010 version. These wavelengths are considered as the minimal scales fully observable  
15 with conventional altimetry, especially with a two-altimeter constellation (Pascual et al, 2006,  
16 Pujol et al. 2005), and thus all the more difficult to interpolate in a 2D grid, at least with  
17 conventional mapping method (Escudier et al, 2013; Dussurget et al, 2011). Moreover, the  
18 spatial grid resolutions used for DT2010 and DT2014 products, as well as the parameters used  
19 for the map construction (e.g. correlation scales), are not adapted for resolving scales smallest  
20 than 100-80 km. The energy associated to these wavelengths drastically fall both for DT2014  
21 and DT2010 products.

22 Compared to the DT2010 products, the new DT2014 version presents more intense geotropic  
23 currents (see Sect. 2.3.3). This has a direct impact on the eddy kinetic energy (EKE) that can  
24 be estimated from the two different versions of the product. The Fig. 10 shows the spatial  
25 differences of the mean EKE deduced from DT2014 and DT2010 products as described in  
26 section 2.3.1. As observed on the SLA variance, the EKE is more important in the DT2014  
27 products, especially in high variability areas where  $+400 \text{ cm}^2/\text{s}^2$  are observed. This  
28 however represents less than 20% of the DT2010 signal. Proportionally, the EKE increase is  
29 quite important in low variability areas and Eastern boundary coastal current where it can  
30 represent below 80% of the DT2010 signal, as underlined by Capet et al (2014). The global  
31 mean EKE increase, excluding the equatorial band and high latitudes areas ( $> \pm 65^\circ\text{N}$ ),  
32 represents nearly 15% of the energy observed in the DT2010 products. This additional energy



1 is induced by different changes implemented in the DT2014 products (see Sect. 2.2.1). Nearly  
2 10% additional energy is the signature of the direct computation of the SLA on the  $1/4^\circ \times 1/4^\circ$   
3 Cartesian grid for DT2014 (see Sect. 2.3.1). The improved mapping parameters, especially  
4 the change of the correlation scales used in the DT2014 products, induce an increase of the  
5 energy of nearly +6%.

### 6 3.2.2 Impact of the altimeter reference period on EKE

7 The Fig. 11 shows the temporal evolution of the Mean EKE over the global ocean both for  
8 DT2014 and DT2010. We first note the nearly 15% additional mean EKE on DT2014 product  
9 as previously discussed. We also note a significant difference of the EKE trend between  
10 DT2014 and DT2010 when the later is kept on the 7-year altimeter reference period (Sect.  
11 2.2.2). Indeed, the mean EKE trend is nearly  $-0.0265$  ( $-0.45$ )  $\text{cm}^2\text{s}^{-2}/\text{year}$  when DT2010\_ref7y  
12 (DT2014) products are considered. At the opposite, when DT2010 is referenced to the 20-  
13 year period, the EKE trend ( $-0.369$   $\text{cm}^2\text{s}^{-2}/\text{year}$ ) is comparable to the DT2014 ( $-0.45$   $\text{cm}^2\text{s}^{-2}/\text{year}$ ).  
14 This result clearly underlines the sensitivity of the EKE trend estimation to the  
15 altimeter reference period used. Indeed, the use of the 20-year reference period leads to a  
16 minimized signature of SLA signal over this period. At the opposite, the SLA gradients are  
17 artificially higher after year 1999 when the historical [1993, 1999] reference period is used.  
18 As a consequences, after year 1999, the EKE deduced from the DT2010 products (let on the  
19 7-year reference period) is higher than the EKE deduced from the DT2014 products (we do  
20 not consider here the global mean EKE bias observed between the two products).

### 21 3.2.3 DT2014 gridded products errors estimation at mesoscales and errors 22 reduction compared to DT2010

23 The accuracy of the gridded SLA products is estimated by comparison with independent  
24 along-track products, focusing on mesoscale signal, as described in section 2.3.2. The results  
25 of the comparison between gridded and along-track products are shown in Fig. 12 and  
26 summarized on Tab. 1.

27 The gridded products errors on mesoscales wavelengths usually range between 4.9 (low  
28 variability area) and 32.5  $\text{cm}^2$  (high variability area), when excluding coastal and high  
29 latitudes areas. They can however be lower, especially on very low variability areas as in the  
30 South Atlantic Sub Tropical gyre (hereafter “reference area”) where the errors observed are  
31 nearly 1.4  $\text{cm}^2$ . It is important to note that these results underline the quality of the “two-sat-





1 merged” gridded products. It can be considered as a degraded product for the mesoscale  
2 mapping since using a minimal altimeter sampling. At the opposite, the “all-sat-merged”  
3 products, during the periods when three or four altimeters were available, benefits from an  
4 improved surface sampling. The errors on these products should thus be lower than observed  
5 on the products merging only two altimeters.

6 Compared to the previous version of the products, the gridded products errors are reduced.  
7 Far from the coast and for ocean variance lower than  $200 \text{ cm}^2$ , the processing/parameters  
8 changes included in the DT2014 version lead to a reduction of nearly 2% of the variance of  
9 the differences between gridded products and along-track measurements observed with  
10 DT2010. The reduction is higher when considering high variability areas ( $> 200 \text{ cm}^2$ ), where  
11 the impact of the new DT2014 processing is maximum. In that case, it reaches nearly -10%.  
12 At the opposite, some slight degradation is observed in the tropic area, especially in the Indian  
13 Ocean. In that region, up to  $1 \text{ cm}^2$  increased variance of the differences between grids and  
14 along-track is observed. This is directly linked with the change of the processing in these  
15 latitudes, especially the reduction of the short wavelength filtering applied before mapping  
16 process, as explained in Sect. 2.2.1.

#### 17 3.2.4 DT2014 Geostrophic currents quality

18 The improved mesoscales mapping also impacts the quality of the geostrophic current  
19 estimated, directly linked to the SLA gradients. Geostrophic currents deduced from ADT  
20 altimeter gridded products were compared with geostrophic currents measured by drifters.  
21 The altimeter and drifter products processing are summarized in sections 2.3.1 and 2.3.3.

22 The distribution of the intensity of the current (not shown), underlines a global  
23 underestimation of the current in the altimeter products compared to the drifters observations,  
24 especially for currents with median and strong intensity ( $> 0.2 \text{ m/s}$ ). However, in both the  
25 cases, the DT2014 currents intensity is still closer to the drifter distribution. The variability of  
26 the current is also increased in the DT2014 dataset to be closer to the observations. The  
27 Taylor skills score (Taylor, 2001) that takes into account both correlation and variability of  
28 the signal is given in Tab. 2. Outside the equatorial band, the Taylor score is 0.83 (0.83) for  
29 zonal (meridian) component. Compared to the DT2010 products it is increased by 0.01 (0.02).

30 The variance reduction of the differences between altimetry and drifters zonal and meridian  
31 components is shown in Fig. 13. The collocated comparisons of zonal and meridian



1 components show that this improvement is not homogeneous in space and that errors in the  
2 position and shape of the structures mapped from altimeter measurements are still observed in  
3 the DT2014 products. Outside the equatorial region ( $\pm 10^\circ\text{N}$ ), the variance reduction observed  
4 with DT2014 product is nearly  $-2.1$  ( $-1.2$ )  $\text{cm}^2/\text{s}^2$  i.e.  $-0.55$  ( $-0.34$ )% of the drifter variance for  
5 zonal (meridian) component. Locally, this reduction can reach more than  $-10\%$ . It is the case  
6 for instance in the Gulf of Mexico and tropical Atlantic Ocean. At the opposite, local  
7 degradation (ranging 2 to 15% of the drifter variance) is observed within the tropics. The  
8 degradation is especially significant in the Pacific (Zonal component), North Indian Ocean  
9 and North of Madagascar. These areas quite well correspond with regions with high  
10 amplitude of M2 internal tide that are still present in the altimeter measurements and affect  
11 the non-tidal signal at wavelength nearly 140km (Dufau et al, 2015). The degradation of the  
12 current seems to underline a noise-like signal in the SLA gridded products. It could  
13 correspond to the signature of this tidal signal, more important in the DT2014 version gridded  
14 products as underlined by Ray et al (2015). This is certainly reinforced by reduced filtering  
15 and the smaller temporal/spatial correlation scales used in this version (Sect. 2.2.1).

### 16 **3.3 Coastal areas and High Latitudes**

17 As described in Sect. 2.2.1, the coastal processing has also been improved. The most visible  
18 impact is the grids spatial coverage in coastal areas greatly improved. The DT2014 grids  
19 indeed better fit with the coastline, as illustrated in Fig. 8 (c, d). This is induced both by the  
20 tuning of the grid definition near the coast, and by the improved definition of the MPs close to  
21 the coast (see Sect. 2.2.1) allowing improved data availability in this area.

22 The grids spatial coverage is also greatly improved In the Arctic region as illustrated in Fig. 8  
23 (a, b). As previously, tuning of the mapping parameters and availability of MPs in this region  
24 directly leads to this result. Additionally, the reduced errors induced by a thinner data  
25 selection and a more precise MP (along ERS-1/2 and EN tracks) used in the DT2014 product  
26 (see Sect. 2.2.1) contribute to reduce the SLA variability as underlined on Fig. 7. In the  
27 Laptev Sea, a local and strong reduction (up to  $100 \text{ cm}^2$ ) of the variance is observed. It is  
28 directly linked with the quality of the MP used (along ERS-1/2 and EN tracks), and also with  
29 the improved data selection (see Sect. 2.2.1), especially for geodetic missions (here mainly C2  
30 en EN after its orbit change) for which precise MP cannot be used.



1 The quality of the gridded products near the coast (0-200km to the coast) was estimated by  
2 comparison with independent along-track measurements as explained in Sect. 2.3.2. Results  
3 are shown in Fig. 12 and Tab. 1. The mean error variance reaches 8.9 cm<sup>2</sup>. It can be more  
4 important in high coastal variability areas, where up to more than 30 cm<sup>2</sup> can be observed  
5 (Indonesian/Philippian coasts, Eastern Australian coasts, Northern Sea coasts and coasts  
6 located at proximity the Western boundary streams). The DT2014 processing induced a  
7 global reduction of these differences compared to the DT2010 products. It reaches 4.1% of  
8 the error variance observed on DT2010 products. However, local degradations are observed,  
9 as along the Philippian coasts.

10 The comparison between gridded products (merging all the altimeters available) and monthly  
11 TG measurements (see Sect. 2.3.3 for methodology) also underlines a global improvement of  
12 the DT2014 products in the coastal areas. The variance of the differences between sea level  
13 observed with altimeter DT2014 gridded products and TG measurements is compared with  
14 the results obtained using the DT2010 gridded products. The results (Fig. 14) show a global  
15 reduction of the variance of the differences between altimetry and TG when DT2014 products  
16 are used. This reduction is quite clear in the Northern coast of the Gulf of Mexico, along the  
17 Indian Eastern coasts and along the US coasts (reduction up to 5 cm<sup>2</sup>, i.e. from 2 and up to  
18 10% of the TG signal). The Western Australian sea level is also better represented in the  
19 DT2014 products (reduction up to 2.5 cm<sup>2</sup> i.e. 1 to 2% of the TGs signal). At the opposite, a  
20 local degradation of the comparison between altimetry and TG is observed in the North  
21 Australian and Indonesian area (augmentation up to 2 cm<sup>2</sup>, with local values reaching up to 5  
22 cm<sup>2</sup>), where it however represents less than 4% of the TGs signal. The local improvements  
23 seen with TGs results are consistent with the conclusion from other diagnosis such as the  
24 comparisons between SLA grids and independent along-track measurements in the same  
25 coastal areas which thus reinforce our confidence in these good results.

### 26 **3.4 Climate scales**

27 Different processing and altimeter standards changes were defined in accordance with the  
28 SL\_cci project and thus also have an impact on the MSL trend estimation especially at  
29 regional scales.

30 The Global MSL trend measured with the DT2014 gridded products over the [1993, 2012]  
31 period is 2.94 mm/year (no GIA applied). The comparison between DT2014 and DT2010



1 products (Fig. 15, b) does not exhibit any differences statistically relevant. Although, no  
2 impact is detected on the Global MSL trend, differences are observed at inter-annual scales  
3 (1-5 years). The main improvement is the ERS-1 calibration during its geodetic phase (i.e.  
4 from April 1994 to March 1995). The nearly 3 mm/year differences observed between  
5 DT2010 and DT2014 during this period traduce an improvement in the DT2014 products.  
6 Indeed, a nearly 6mm bias between ERS-1 and TP were observed in the DT2010 product and  
7 not entirely reduced when merging both the altimeter measurements. This was corrected in  
8 the DT2014 version. Fig. 15 (b) also underlines a global 5.5 mm mean bias difference  
9 between the mean SLA form DT2014 and DT2010. This bias is directly linked to the global  
10 SLA reference convention used in the DT2014 version as explained in Sect. 2.2.2.

11 The regional MSL trend differences between DT2014 and DT2010 (Fig. 15, a) are similar to  
12 the differences underlined by Philipps et al, (2013a and 2013b) and Ablain et al (2015)  
13 between SL\_cci and DT2010 products (see fig 6 of the paper). As explained by the authors,  
14 the change of the orbit standards solution mainly explains the East/West dipole differences.

15 In order to highlight the improved regional MSL trend estimation with DT2014 product at  
16 such hemispheric scales, the trend deduced from altimeter products were compared to the  
17 trend deduced from in-situ T/S profiles (see Sect. 2.3.3 for processing). This comparison was  
18 done during the [2005, 2012] period when a significant number of in-situ measurements are  
19 available. One should expect homogeneous differences between altimeter and in-situ  
20 measurements in both hemispheres. It is the case for DT2014 products for which the MSL  
21 trend differences reach nearly 1.56 (1.68) mm/year in the Eastern (Western) hemisphere. In  
22 the opposite, an unhomogeneity is observed with DT2010 since the MSL trend differences  
23 with in-situ measurements are 2.02 (1.05) mm/year, underlining the nearly 1 mm MSL trend  
24 differences between both hemispheres.

25 As underlined in Ablain et al (2015), the regional MSL trend comparison also show  
26 differences at smaller scales. Here again, the change of some standards are directly  
27 responsible for these differences. The use of the ERA-Interim meteorological fields in the  
28 DAC solution (see Sect.2.1) mainly impact the regional MSL trend estimation in the southern  
29 high latitudes areas, as underlined by Carrere et al. (2015). The same meteorological forcing  
30 used in the wet troposphere correction slightly contributes to the regional improvement of the  
31 MSL trend, especially for the first decade (Legeais et al 2014). Part of the smallest regional  
32 scales differences are also induced by the improved inter-calibration processing in the



1 DT2014 products, better taking into account the regional biases from a reference mission to  
2 the other (see Sect. 2.2.1).

3 Some improvements implemented in the DT2014 version also impact the interannual signal  
4 reconstruction at regional scales. The more accurate estimation of the LWE associated to the  
5 ionospheric signal correction (see Sect. 2.2.1) leads to a reduced signature of these errors in  
6 the products especially during the period of high solar activity. It was the case in 2000, when  
7 ERS-2 measurement is not done on a dual-frequency mode that prevent us from estimating a  
8 precise ionospheric correction. The additional LWE in the polar equatorial band, induced by  
9 the use of a less precise model solution, are taken into account in the DT2014 products. The  
10 comparison of the regional mean SLA from ERS-2 measurements with TP (for which precise  
11 ionospheric correction is available) over the year 2000 (Fig. 16) underlines a residual  
12 ionospheric signal that locally reaches 5 mm. The same comparison done with DT2010  
13 products shows that this residual error was quite two time more stronger in this version with  
14 locally more than 1 cm bias between ERS-2 and TP measurements.

15

#### 16 **4 Discussions and Conclusions**

17 For the first time, more than 20 years of altimeter L3 to L4 products were entirely reprocessed  
18 and delivered as the DT2014 version. This reprocessing takes into account the last altimeter  
19 standards, and also includes important changes of different parameters/methods involved at  
20 each step of the processing. At the end, the changes implemented impact the signal at  
21 different spatial and temporal scales, from large to mesoscales and from low to high  
22 frequency.

23 One important change consists in referencing the SLA products on a new altimeter reference  
24 period, taking advantage of the 20 years of measurements available and leading to a more  
25 realistic signature of SLA interannual signal. The variability of the SLA, as well as the EKE  
26 deduced from SLA gradients is thus changed compared to the DT2010 dataset, especially  
27 after 1999. This change is visible on the mean EKE trend over the 20 year period,  
28 overestimated in DT2010. This impact suggests that previous estimations of EKE trend from  
29 altimeter products (e.g. Pujol et al, 2005 ; Hogg et al., 2015) should be reviewed taking into  
30 account the altimeter reference period.



1 The DT2014 dataset is more energetic than the DT2010. The variability of the signal is  
2 increased by 5.1% in the DT2014 products, underlining additional signal for wavelengths  
3 lower than ~250 km. A global EKE 15% increase (equatorial band excluded) is also observed  
4 with DT2014. This increase is higher in low variability and eastern coastal areas where it  
5 reaches up to 80%. The direct computation of the DT2014 products on the  $\frac{1}{4}^\circ \times \frac{1}{4}^\circ$  Cartesian  
6 grid explains nearly 2/3 of variability/energy increase. The other 1/3 is directly linked with  
7 the improved parameterization of the mapping processing. Contrary to the DT2010  
8 reprocessing (Dibarboure et al, 2011), the impact of the altimeter standards is moderate in  
9 comparison with the impact of the processing changes. The improved accuracy of the along-  
10 track signal, induced by the use of more accurate altimeter standards (see Sect.2.1) should  
11 contribute to reduce the SLA error variance observed with gridded products. It was the case  
12 when comparing DT2010 with previous DT2007 gridded products (Dibarboure et al, 2011).  
13 The DT2010 products did not include significant changes in the mapping processing, and the  
14 reduction of SLA error variance, more important in the Indonesian area, was mainly  
15 explained by the use of improved altimeter GDR-C standards. However, the amplitude of this  
16 error variance reduction is quite 10 times less important than the impact of the mapping  
17 processing changes implemented in the DT2014 products.

18 The additional signal observed in DT2014 traduces the improved signal reconstruction,  
19 especially at mesoscales, as previously underlined by Capet et al (2014) in the Eastern  
20 boundary upwelling systems. The DT2014 products quality was estimated at global scales  
21 using comparison with independent measurements (altimetry and in-situ) which allowed us to  
22 establish a refined mesoscales error budget given for the merged gridded products. The  
23 DT2014 SLA products errors for mesoscales signal in open ocean is estimated between 1.5  
24  $\text{cm}^2$  in low variability areas and up to 33 $\text{cm}^2$  in high variability areas where the altimeter  
25 sampling does not allow a full observation of the SLA variability. Compared to the previous  
26 version of the products, this error is reduced by a factor up to 10% in high variability areas.

27 The geostrophic currents are globally slightly intensified in the DT2014 products, becoming  
28 closer to the surface drifters observations. The geostrophic current however is still globally  
29 underestimated compared to the in-situ observations. Outside the tropical band, the variance  
30 of the differences between altimeter products and in-situ observations is reduced almost  
31 everywhere. This reduction locally reaches up to 10% of the in-situ variance. At the opposite,  
32 geostrophic current estimated with DT2014 products is globally lower correlated with in-situ



1 observation within the tropics. This degradation locally represents up to 15% of the in-situ  
2 variance.

3 DT2014 products were also improved in coastal and high latitude areas. The main  
4 improvement is visible on the spatial coverage, refined in coastal areas and improved in  
5 Arctic region with a better definition of the coastline and sea ice edge. The errors of SLA  
6 gridded products in the coastal areas (< 200km) are estimated nearly 9 cm<sup>2</sup>, with higher  
7 values in high variability coastal areas. This error is globally reduced by 4% compared to the  
8 previous version of the products. The consistency with TGs measurements is improved  
9 especially in different areas such as the Northern coast of the Gulf of Mexico, along the  
10 Indian Eastern coasts and along the US coasts. In that case the reduction of variance of the  
11 differences between altimetry and TGs ranges between 2 and up to 10 % of the TGs signal  
12 when compared to the results obtained with DT2010 products. In some other coastal areas,  
13 degradation is however underlined. It is the case in the North Australian and Indonesian area  
14 where it reaches less than 4% of the TGs signal.

15 The quality of the regional products is not specifically addressed in this paper. However, as  
16 for the global products, mapping was also improved at regional scale with a positive impact in  
17 coastal areas, as underlined by Marcos et al (2015) and Juza et al (2015, in preparation) in the  
18 Mediterranean Sea.

19 Globally, the comparison to different independent measurements gives consistent results,  
20 highlighting improvement or degradation in the same areas, reinforcing our confidence in  
21 these results.

22 The climate scales are also improved with DT2014, taking advantage of the altimeter  
23 standards and processing defined in consistency with SL\_cci project. The global MSL trend  
24 estimation is nearly unchanged in the DT2014 products compared to the DT2010. However,  
25 significant improvements are underlined at regional scales, with a reduction of the  $\pm 1$ mm/year  
26 dipole error observed in the DT2010 between eastern and western basin. Additionally, the  
27 residual ionospheric errors, previously observed on altimeter measurements without dual-  
28 frequency, are reduced by up to 50% in the DT2014 products.

29

30 The assessment of the quality of the DT2014 products at mesoscales underlined the limits of  
31 the products.



1 First, the spectral content of the gridded products clearly underlines that part of the small  
2 signal is missing in the gridded products. Finally, the mean spatial resolution of the products  
3 was estimated to be nearly  $1.7^\circ$  i.e.  $\sim 150$  km at mid latitudes (Chelton et al, 2014). The  
4 comparison with the spectral content deduced from full resolution along-track measurements  
5 (not shown) underlines that nearly 21 cm<sup>2</sup> of the global ocean variance is missed with gridded  
6 products (wavelengths  $< 65$ km excluded; comparison with AL 1 Hz measurements over year  
7 2013). It represents nearly 16% of the along-track signal and up to 40% when wavelengths  
8 ranging 300-65km are considered. In other words, nearly 2/5 of the mesoscale variability is  
9 missed with DT2014 gridded products. This is clearly linked to the mapping methodology,  
10 combined with altimeter constellation sampling capabilities.

11 The second limit of the DT2014 product is the additional non mesoscale signal that is  
12 observed. It is characteristic of the residual M2 internal tide visible on both along-track  
13 (Dufau et al, 2015) and gridded products (Ray et al, 2015). The presence of this signal leads  
14 to local degradation of the DT2014 quality in specific areas. The signature of the internal  
15 waves is on the same wavelengths than mesoscale signal DUACS products focus on, making  
16 tricky the reduction of this signal without affecting mesoscale signal.

17

18 In spite of these limitations, the quality and accuracy of the DUACS products makes them  
19 valuable for many applications. They are currently used for derived oceanographic products  
20 generation like ocean indicators (e.g. regional MSL; ENSO; Kuroshio among others;  
21 <http://www.aviso.altimetry.fr>). They are also currently used for the generation of lagrangian  
22 products, for which the precision of the current can strongly impact the results (d'Ovidio et  
23 al, 2015).

24 In order to ensure the best homogeneity and quality, the DUACS DT products will be  
25 regularly reprocessed for all missions, taking advantage of the new altimeter standards and  
26 L3/L4 improved processing. The next reprocessed version of the products will be performed  
27 as part of the new European Copernicus Marine Environment Marine Service (CMEMS) and  
28 is expected for 2018.

29

30 **Appendix A: How to change the reference period**





1 The gridded SLA products can be referenced to another reference period following the Eq.  
2 (1), where P and N are two different reference periods and  $\langle SLA \rangle_X$  is the temporal mean of the  
3 SLA over the period X. In the same way, MSS and MDT can be referenced to different  
4 reference period following eq (2) and (3).

$$5 \quad SLA_P = SLA_N - \langle SLA_N \rangle_P \quad (1)$$

$$6 \quad MSS_P = MSS_N + \langle SLA_N \rangle_P \quad (2)$$

$$7 \quad MDT_P = MDT_N + \langle SLA_N \rangle_P \quad (3)$$

8 By definition, the ADT is independent of the reference period. ADT is obtained combining  
9 SLA and MDT defined over the same reference period (eq. 4)

$$10 \quad ADT = SLA_N + MDT_N = SLA_P + MDT_P \quad (4)$$

11

## 12 Acknowledgements

13 The DT2014 reprocessing exercise has been supported by the French SALP/CNES project  
14 with co-funding from European MyOcean-2 and MyOcean Follow On projects. The dataset  
15 are available on the Aviso website ([http](http://www.aviso.oceanobs.com/)) and the CMEMS web site ([http](http://www.cmems.eu/)). Level 2 (GDR)  
16 input data are provided by CNES, ESA, NASA. The altimeter standards used in DT2014 were  
17 selected taking advantage of the work performed in the first phase of the Sea Level Climate  
18 Change Initiative (SL\_cci) led by the ESA in 2011-2013

19

20

21

22



## 1 **References**

- 2 Ablain, M., . Cazenave, G. Valladeau, and S. Guinehut, A new assessment of the error budget  
3 of global mean sea level rate estimated by satellite altimetry over 1993-2008. Ocean Science,  
4 5, 193-201, 2009.
- 5 Ablain M., A. Cazenave, G. Larnicol, M. Balmaseda, P. Cipollini, Y. Faugère, M. J.  
6 Fernandes, O. Henry, J. A. Johannessen, P. Knudsen, O. Andersen, J. Legeais, B.  
7 Meyssignac, N. Picot, M. Roca, S. Rudenko, M. G. Scharffenberg, D. Stammer, G. Timms,  
8 and J. Benveniste, Improved sea level record over the satellite altimetry era (1993–2010) from  
9 the Climate Change Initiative project, Ocean Science., 11, 67-82, doi:10.5194/os-11-67-2015,  
10 2015.
- 11 Arbic B. K, Scott R. B., Chelton D. B., Richman J. G. and Shriver J. F., Effects on stencil  
12 width on surface ocean geostrophic velocity and vorticity estimation from gridded satellite  
13 altimeter data, J. Geophys. Res., vol117, C03029, doi:10.1029/2011JC007367, 2012.
- 14 AVISO/DUACS, A new version of SSALTO/Duacs products available in April 2014.  
15 Technical note. Available at  
16 <http://www.aviso.altimetry.fr/fileadmin/documents/data/duacs/Duacs2014.pdf>, last access:  
17 2015/12/07, 2014a.
- 18 AVISO/DUACS, User Handbook Ssalto/Duacs: M(SLA) and M(ADT) Near-Real Time and  
19 Delayed-Time, SALP-MU-P-EA-21065-CLS, edition 4.1, May 2014, available at  
20 [http://www.aviso.altimetry.fr/fileadmin/documents/data/tools/hdbk\\_duacs.pdf](http://www.aviso.altimetry.fr/fileadmin/documents/data/tools/hdbk_duacs.pdf), last access:  
21 2015/12/07, 2014b.
- 22 Capet A., E. Mason, V. Ross, C. Troupin, Y. Faugere, M.-I. Pujol, A. Pascual, Implications  
23 of a Refined Description of Mesoscale Activity in the Eastern Boundary Upwelling Systems,  
24 Geophys. Res. Lett., 41, doi:10.1002/2014GL061770, 2014.
- 25 Carrere L. and M. Ablain, Major improvement of altimetry sea level estimations using  
26 pressure derived corrections based on ERA-interim atmospheric reanalysis, 2015, in  
27 preparation.
- 28 Chelton D., G. Dibarboure , M.-I. Pujol, G. Taburet , M. G. Schlax, The Spatial Resolution of  
29 AVISO Gridded Sea Surface Height Fields, OSTST Lake Constance, Germany, October, 28-  
30 31 2014, available at



- 1 [http://meetings.aviso.altimetry.fr/fileadmin/user\\_upload/tx\\_ausycslseminar/files/29Red0900-](http://meetings.aviso.altimetry.fr/fileadmin/user_upload/tx_ausycslseminar/files/29Red0900-)  
2 [1\\_OSTST\\_Chelton.pdf](#), 2014
- 3 Dibarboure G., M.-I. Pujol, F. Briol, P.-Y. Le Traon, G. Larnicol, N. Picot, F. Mertz, P.  
4 Escudier, M. Ablain, and C. Dufau, Jason-2 in DUACS: first tandem results and impact on  
5 processing and products, *Mar. Geod.*, OSTM Jason-2 Calibration/Validation Special Edition –  
6 Part 2 Jason-2 Special Edition – Part 2, (34), 214-241, 2011,  
7 doi:10.1080/01490419.2011.584826
- 8 F. d'Ovidio, A. Della Penna, T. W. Trull, F. Nencioli, M.-I. Pujol, M.-H. Rio, Y.-H. Park, C.  
9 Cotté, M. Zhou, and S. Blain, The biogeochemical structuring role of horizontal stirring:  
10 Lagrangian perspectives on iron delivery downstream of the Kerguelen Plateau,  
11 *Biogeosciences*, 12, 5567-5581, 2015
- 12 Ducet N., Le Traon P.-Y., Reverdun G., Global high-resolution mapping of ocean circulation  
13 from TOPEX/Poseidon and ERS-1 and -2, *J. Geophys. Res.* 105 (C8), 19,477-19,498, 2000
- 14 Dufau C., M. Orstynowicz, G. Dibarboure, R. Morrow, P.-Y. La Traon, (2014): Mesoscale  
15 Resolution Capability of altimetry: present & future, *J. Geophys. Res.*, 2015, in review
- 16 Dussurget R., F. Birol, R. Morrow and P. De Mey, Fine Resolution Altimetry Data for a  
17 Regional Application in the Bay of Biscay, *Mar. Geod.*, 34:3-4, 447-476, 2011
- 18 Escudier, R., J. Bouffard, A. Pascual, P.-M. Poulain, and M.-I. Pujol, Improvement of coastal  
19 and mesoscale observation from space: Application to the northwestern Mediterranean Sea,  
20 *Geophys. Res. Lett.*, 40, 2148–2153, doi:10.1002/grl.50324, 2013.
- 21 Fieguth P, D. Menemenlis, T. Ho, A. Willsky, C. Wunch, Mapping Mediterranean  
22 Altimeter Data with a Multiresolution Optimal Interpolation Algorithm, *J. Atmos. Oceanic*  
23 *Technol.*, 15,535-546, 1998
- 24 Griffin D and M Cahill, Assessment of Cryosat near-real-time sea level anomaly data using  
25 HF radar and SST imagery, Oral presentation, OSTST Venice, Italy 2012, available at  
26 [http://www.aviso.altimetry.fr/fileadmin/documents/OSTST/2012/oral/01\\_thursday\\_27/06\\_NR](http://www.aviso.altimetry.fr/fileadmin/documents/OSTST/2012/oral/01_thursday_27/06_NRT_applications/07_NRT_Griffin.pdf)  
27 [T\\_applications/07\\_NRT\\_Griffin.pdf](#), 2012.
- 28 Hogg, A. McC., M. P. Meredith, D. P. Chambers, E. P. Abrahamson, C. W. Hughes, and A.  
29 K. Morrison, Recent trends in the Southern Ocean eddy field, *J. Geophys. Res. Oceans*, 120,  
30 257–267, doi:10.1002/2014JC010470, 2015.



- 1 Jayne S., B.Owens, B. Cornuelle, Mapping the ocean's surface circulation from altimetry,  
2 Oral presentation, OSTST Boulder USA 2013, available at  
3 <http://www.aviso.altimetry.fr/fileadmin/documents/OSTST/2013/oral/Jayne.pdf>, 2013
- 4 Juza M., R. Escudier, A. Pascual, M.-I. Pujol, C. Troupin, B. Mourre, J. Tintoré, Impact of the  
5 reprocessed satellite altimetry absolute dynamic topography on the Western Alboran Gyre  
6 variability, 2015, in preparation.
- 7 Leben R R, G H Born, B N Engebret, Operational Altimeter Data Processing for Mesoscale  
8 Monitoring, *Mar. Geod.*, 25:3–18, 2002
- 9 Legeais J.-F., P. Prandi, M. Ablain, Validation of altimeter data by comparison with in-situ  
10 T/S Argo profiles, Ref. CLS/DOS/NT/15-007, available at  
11 [http://www.aviso.altimetry.fr/fileadmin/documents/calval/validation\\_report/annual\\_report\\_insitu\\_TS\\_2014.pdf](http://www.aviso.altimetry.fr/fileadmin/documents/calval/validation_report/annual_report_insitu_TS_2014.pdf), last access: 2015/12/07, 2015
- 12
- 13 Legeais, J.-F., Ablain, M., and Thao, S.: Evaluation of wet troposphere path delays from  
14 atmospheric reanalyses and radiometers and their impact on the altimeter sea level, *Ocean*  
15 *Sci.*, 10, 893– 905, doi:10.5194/os-10-893-2014, 2014.
- 16 Le Traon P.Y. and Hernandez F., Mapping of the oceanic mesoscale circulation: validation of  
17 satellite altimetry using surface drifters. *J. Atmos. Oceanic Technol.*, 9, 687-698, 1992.
- 18 Le Traon P.-Y., Gaspar P., Bouyssel F., and Makhmara H., Using TOPEX/Poseidon data to  
19 enhance ERS-1 data, *J. Atmos. Oceanic Technol.*, 12, 161-170, 1995.
- 20 LeTraon P.-Y., G Dibarboure, Mesoscale Mapping Capabilities of Multiple-Satellite  
21 Altimeter Missions, *J. Atmos. Oceanic Technol.*, 16, 1208-1223, 1999.
- 22 LeTraon P.-Y, Y. Faugere, F. Hernamdez, J. Dorandeu, F. Mertz and M. Abalin, Can We  
23 Merge GEOSAT Follow-On with TOPEX/Poseidon and ERS-2 for an Improved Description  
24 of the Ocean Circulation?, *J. Atmos. Oceanic Technol.*, 20, 889-895, 2003
- 25 Marco M., A. Pascual, M-I Pujol, Improved satellite altimeter mapped sea level anomalies in  
26 the Mediterranean Sea: A comparison with tide gauges, *Advances in Space Research* 56 (4),  
27 596–604. doi:10.1016/j.asr.2015.04.027, 2015
- 28 Mulet S., M.H. Rio, E. Greiner, N. Picot, A. Pascual, New global Mean Dynamic Topography  
29 from a GOCE geoid model, altimeter measurements and oceanographic in-situ data, OSTST  
30 Boulder USA 2013, available at



- 1 [http://www.aviso.altimetry.fr/fileadmin/documents/OSTST/2013/oral/mulet\\_MDT\\_CNES\\_C](http://www.aviso.altimetry.fr/fileadmin/documents/OSTST/2013/oral/mulet_MDT_CNES_C)  
2 LS13.pdf, 2013.
- 3 Pascual A., Faugere Y., Larnicol G., Le Traon P.-Y., Improved description of the ocean  
4 mesoscale variability by combining four satellite altimeters, *Geophys. Res. Lett.*, 33(2),  
5 doi:10.1029/2005GL024633, 2006
- 6 Philipps S., H. Roinard, N. Picot, Jason-2 reprocessing impact on ocean data (cycles 001 to  
7 145), Ref. CLS/DOS/NT/12-222., available at  
8 [http://www.aviso.altimetry.fr/fileadmin/documents/calval/validation\\_report/J2/Jason2ReprocessingReport-v2.1.pdf](http://www.aviso.altimetry.fr/fileadmin/documents/calval/validation_report/J2/Jason2ReprocessingReport-v2.1.pdf), last access: 2014/12/07, 2013a.
- 10 Philipps S., H. Roinard, N. Picot, (2013b): Jason-1 validation and cross calibration activities  
11 [Annual Report 2013], Ref. CLS/DOS/NT/13-226., available at  
12 [http://www.aviso.altimetry.fr/fileadmin/documents/calval/validation\\_report/annual\\_report\\_j1\\_2013.pdf](http://www.aviso.altimetry.fr/fileadmin/documents/calval/validation_report/annual_report_j1_2013.pdf), last access: 2014/07/25, 2013b.
- 14 Pujol M.-I. and G. Larnicol, Mediterranean Sea eddy kinetic energy variability from 11 years  
15 of altimetric data, *J. Mar. Syst.*, 58 (3–4) (2005), 121–142, 2005.
- 16 Ray R.D. and Zaron E.D., M2 internal tides and their observed wavenumber spectra from  
17 satellite altimetry, *Journal of Physical Oceanography*, doi: 10.1175/JPO-D-15-0065.1, in  
18 press., 2015.
- 19 Rio, M. H., S. Guinehut, and G. Larnicol, New CNES-CLS09 global mean dynamic  
20 topography computed from the combination of GRACE data, altimetry, and in-situ  
21 measurements, *J. Geophys. Res.*, 116, C07018, doi:10.1029/2010JC006505, 2011.
- 22 Rio, M-H, Use of altimeter and wind data to detect the anomalous loss of SVP-type drifter's  
23 drogue. *J. Atmos. Oceanic Technol.*, DOI:10.1175/JTECH-D-12-00008.1, 2012.
- 24 Schaeffer P., Y. Faugere, J. F. Legeais, A. Ollivier, T. Guinle, N. Picot, The CNES CLS11  
25 Global Mean Sea Surface Computed from 16 Years of Satellite Altimeter Data. *Mar. Geod.*,  
26 Special Issue, Jason-2, Vol.35, 2012.
- 27 Taylor, K. E., Summarizing multiple aspects of model performance in a single diagram, *J.*  
28 *Geophys. Res.*, 106(D7), 7183–7192, doi:10.1029/2000JD900719, 2001.
- 29 Valladeau G., J.-F. Legeais, M. Ablain, S. Guinehut, N. Picot, Comparing Altimetry with  
30 Tide Gauges and Argo Profiling Floats for Data Quality Assessment and Mean Sea Level



- 1 Studies, Marine Geodesy, OSTM Jason-2 Applications Special Edition – Part 3, (35), 42-60,
- 2 doi:10.1080/01490419.2012.718226, 2012
- 3 Prandi P., G. Valladeau G., M. Ablain, Validation of altimeter data by comparison with tide
- 4 gauge measurements, Ref. CLS/DOS/NT/15-020, available at
- 5 [http://www.aviso.altimetry.fr/fileadmin/documents/calval/validation\\_report/annual\\_report\\_ins](http://www.aviso.altimetry.fr/fileadmin/documents/calval/validation_report/annual_report_insitu_TG_2014.pdf)
- 6 [itu\\_TG\\_2014.pdf](http://www.aviso.altimetry.fr/fileadmin/documents/calval/validation_report/annual_report_insitu_TG_2014.pdf), last access: 2015/12/07, 2015.
- 7



1 Table 1: Variance of the differences between gridded DT2014 two-sat-merged products and  
 2 independent TPN along-track measurements for different geographic selections (unit = cm<sup>2</sup>).  
 3 In parenthesis: variance reduction (in %) compared with the results obtained with the DT2010  
 4 products. Statistics are presented for wavelength ranging 65-500 km and after latitude  
 5 selection ( $|\text{LAT}| < 60^\circ$ ).

	<b>TPN [2003,2004]</b>
<b>Reference area*</b>	1.4 (-0.7%)
<b>Dist coast &gt; 200km &amp; variance &lt; 200 cm<sup>2</sup></b>	4.9 (-2.1%)
<b>Dist coast &gt; 200km &amp; variance &gt; 200 cm<sup>2</sup></b>	32.5 (-9.9%)
<b>Dist coast &lt; 200km</b>	8.9 (-4.1%)

6 *\*The reference area is defined by [330,360°E]; [-22,-8°N]*

7



1 Table 2: Taylor skill score of the comparison of the geostrophic current deduced from  
2 altimetry or measured by drifters. Results obtained with DT2014 (2010) products are in bold  
3 (parenthesis).

	Zonal	Meridian
Outside the equatorial band	<b>0.83</b> (0.82)	<b>0.62</b> (0.63)
Inside the equatorial band	<b>0.87</b> (0.85)	<b>0.83</b> (0.81)

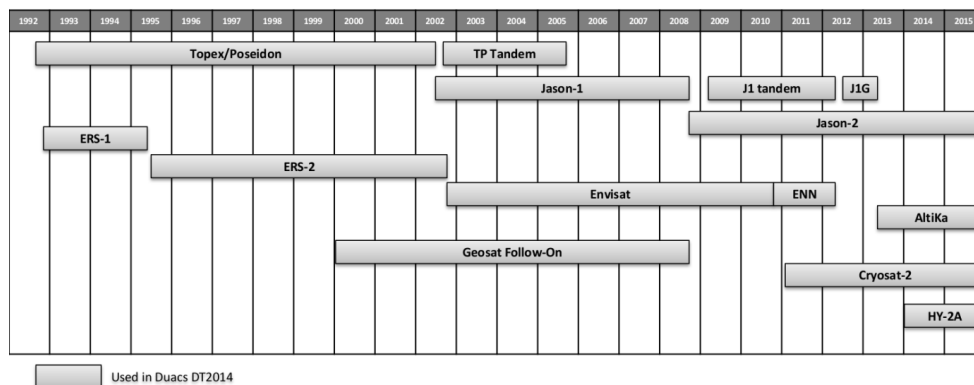
4

5





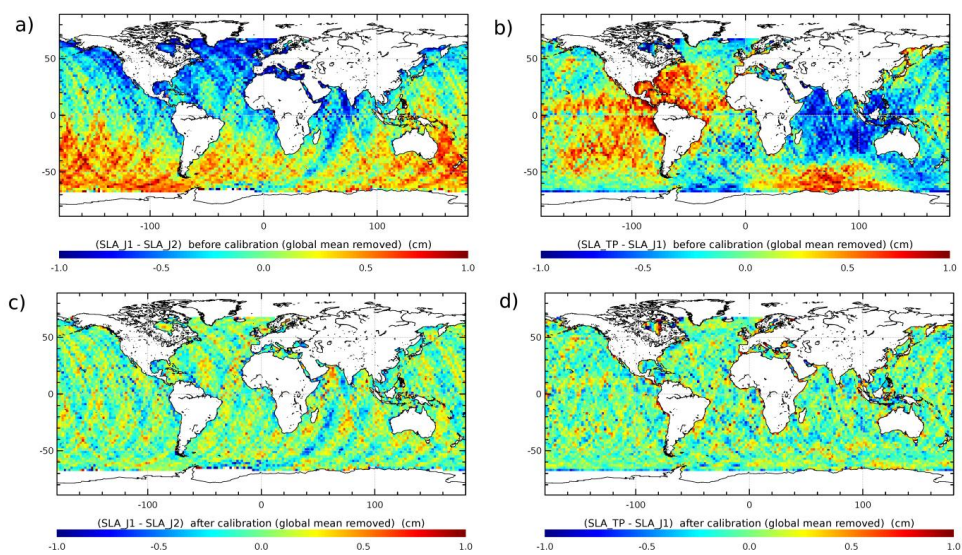
1



2

3 Figure 1 : Timeline of the altimeter missions used (or expected) in the multi-mission DUACS  
4 DT system.

5



1

2 Figure 2 : Regional biases observed between TP and J1 during the cycles 1 to 21 of J1 before

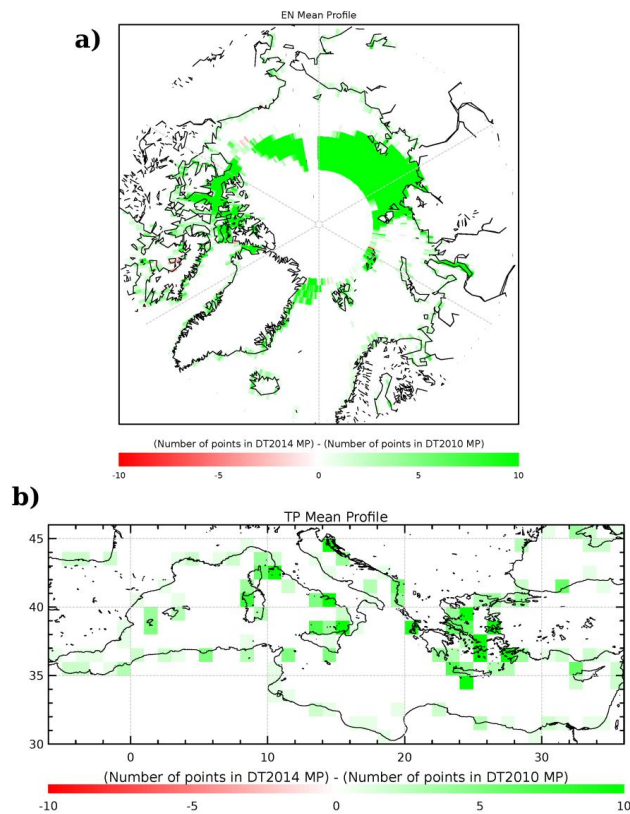
3 (a) and after (c) reduction of the biases. Regional biases observed between J1 and J2 during

4 the cycles 1 to 21 of J2, before (b) and after (d) reduction of the biases.

5



1



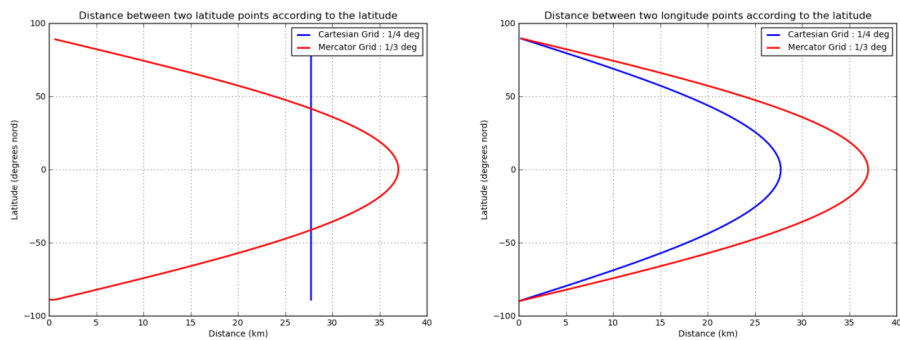
2

3 Figure 3: Differences of the number of points defined along the new and old version of the  
4 Mean Profile defined along EN (a) and TP (b) theoretical tracks. Statistics done in 1°x1°  
5 boxes.

6



1



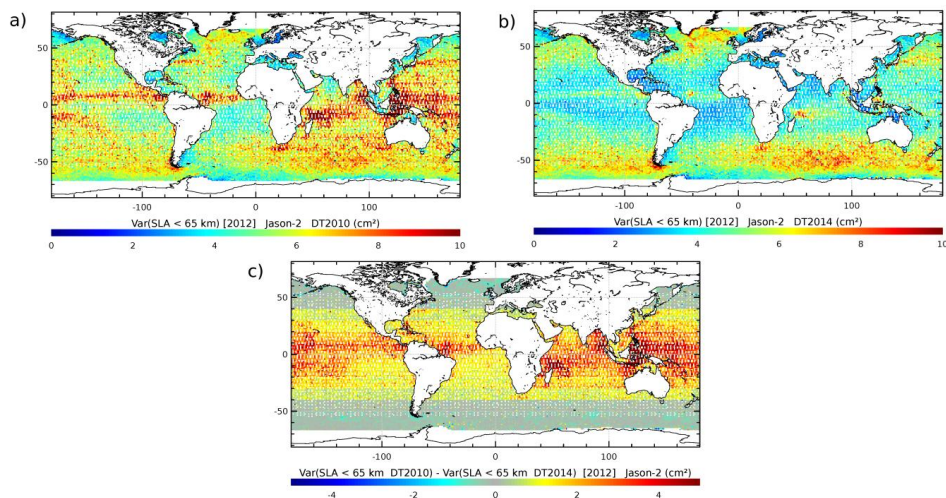
2

3 Figure 4 : Left : Difference between two successive grid points on a meridian section as a  
4 function of the latitude, for a  $1/4^\circ \times 1/4^\circ$  Cartesian resolution (blue) and  $1/3^\circ \times 1/3^\circ$  Mercator  
5 resolution (red). Right: same as left but for a zonal section.

6



1



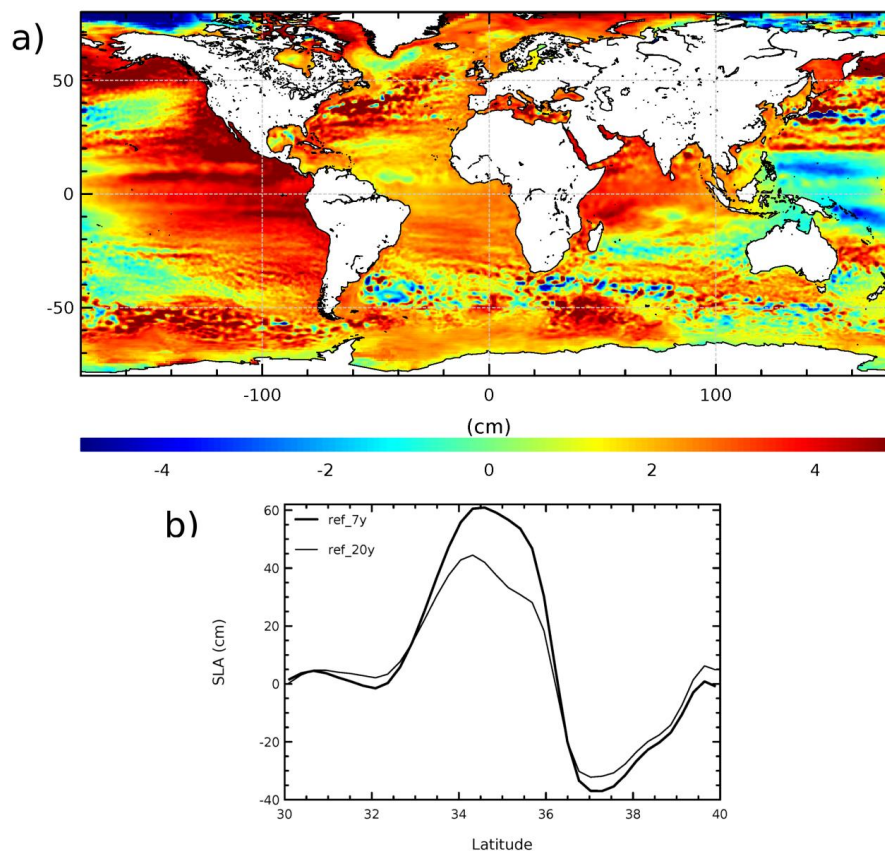
2

3

Figure 5 : Variance of the short wavelength signal filtered on along-track J2 products in the  
DT2010 (a) and DT2014 (b) versions. Differences between the two maps (c). Statistics done  
over year 2012.

6

7



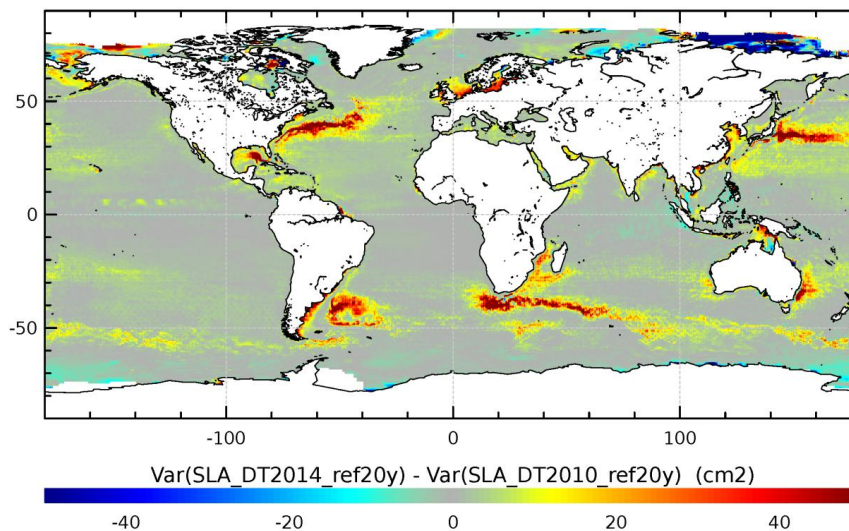
1

2 Figure 6 : Impact of the change of reference period. a) regional MSL variation differences  
3 when considering the 7-year or the 20-year period. b) SLA along a J2 track crossing the  
4 Kuroshio, referenced to the 7-year (red) and 20-year (bleu) period.

5



1



2

3 Figure 7: Difference between SLA variance observed with DT2014 gridded products and

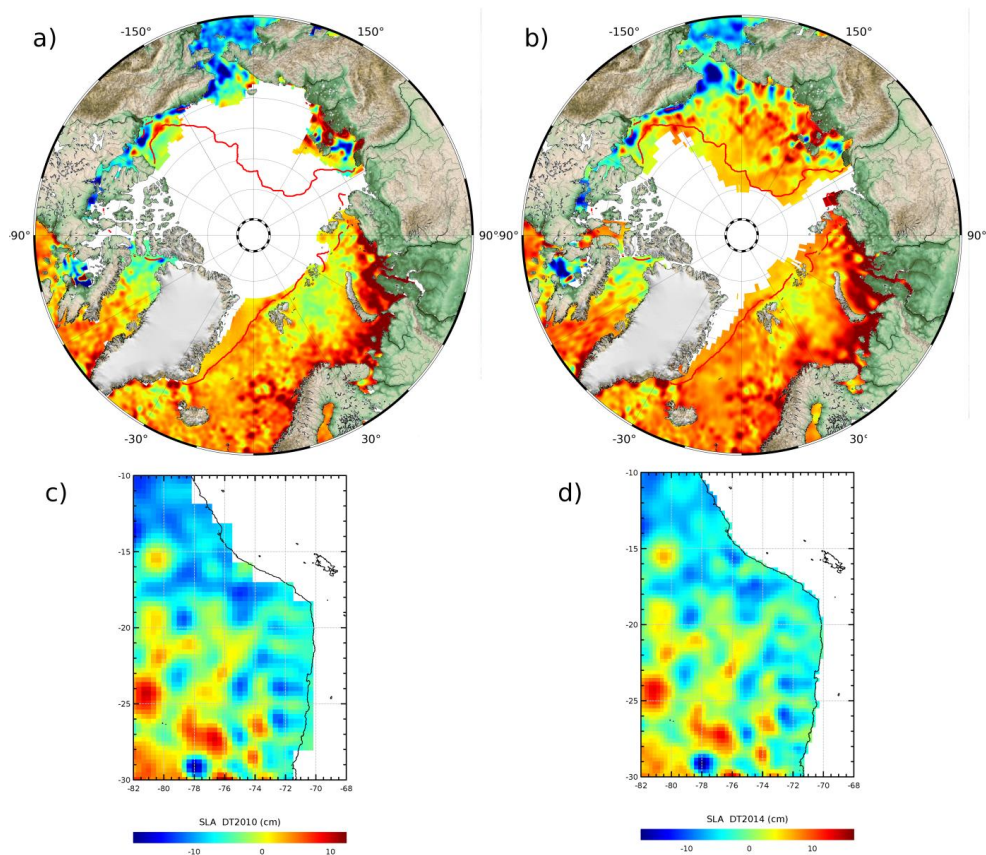
4 SLA variance observed with DT2010 products over the [1993, 2012] period. Gridded

5 products merging all the altimeters available are considered (i.e. “all-sat-merged” in DT2014;

6 “UPD” in DT2010). DT2010 products were referenced to the 20-year altimeter reference

7 period and interpolated on the  $\frac{1}{4}^\circ \times \frac{1}{4}^\circ$  Cartesian grid for comparison with DT2014.

8

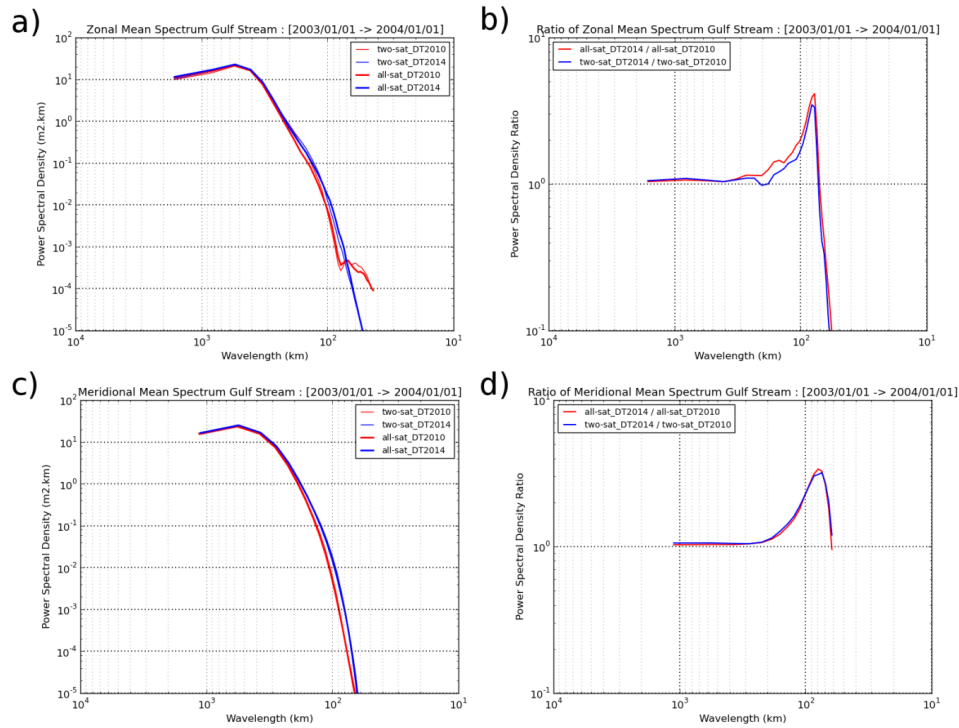


1

2 Figure 8: Coverage improvement associated with the DT2014 reprocessing. Map of SLA for  
3 day 2011/10/17 over the Arctic Ocean observed with DT2010 (a) and DT2014 (b) product.  
4 Sea ice edge is underlined with red line (OSISAF product). Same map along the Western  
5 South- American coast with DT2010 (c) and DT2014 (d).

6



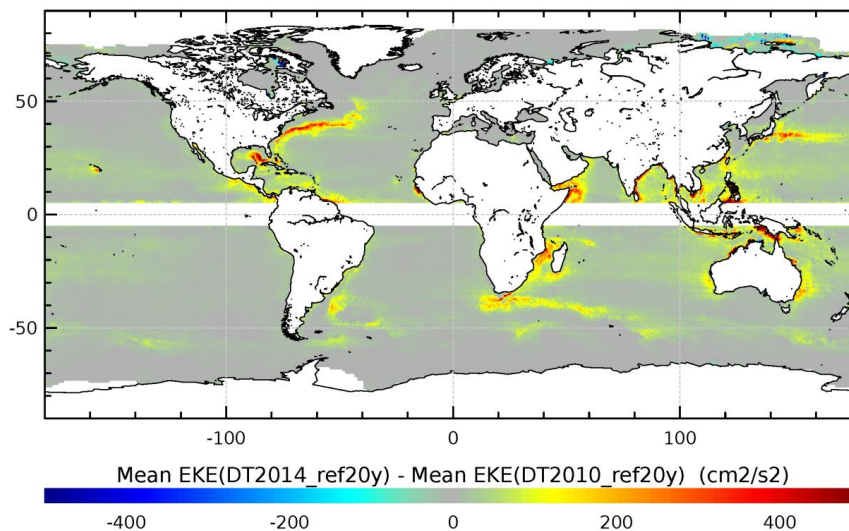


1  
2  
3  
4  
5  
6  
7  
8

Figure 9: Mean zonal (a) and meridian (c) power spectral density deduced from gridded DT2014 (blue) and DT2010 (red) all-sat-merged (UPD; thick line) and two-sat-merged (REF; thin line) products over the Gulf Stream area during the year 2003 (when the constellation included J1, TP Tandem, Geosat Follow On and EN). Ratio between DT2010 and DT2014 products when all-sat-merged (UPD; thick line) and two-sat-merged (REF; thin line) are considered: zonal (b) and meridian (d) component..



1



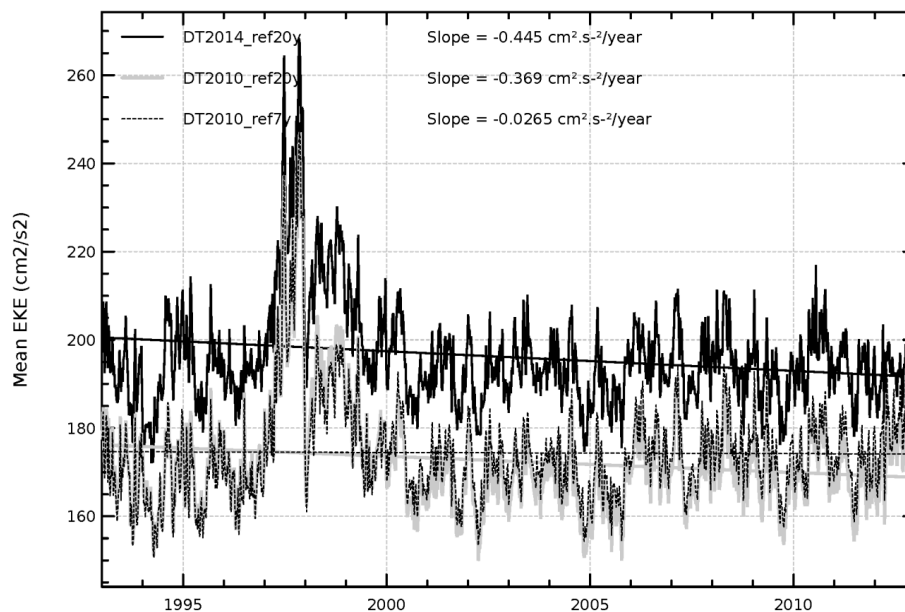
2

3 Figure 10: Difference of the mean EKE between DT2014 and DT2010 products over the  
4 [1993, 2012] period. Gridded products merging all the altimeters available are considered (i.e.  
5 “all-sat-merged” in DT2014; “UPD” in DT2010). DT2010 products were referenced to the  
6 20-year altimeter reference period and interpolated on the  $\frac{1}{4}^\circ \times \frac{1}{4}^\circ$  Cartesian grid for  
7 comparison with DT2014

8



1



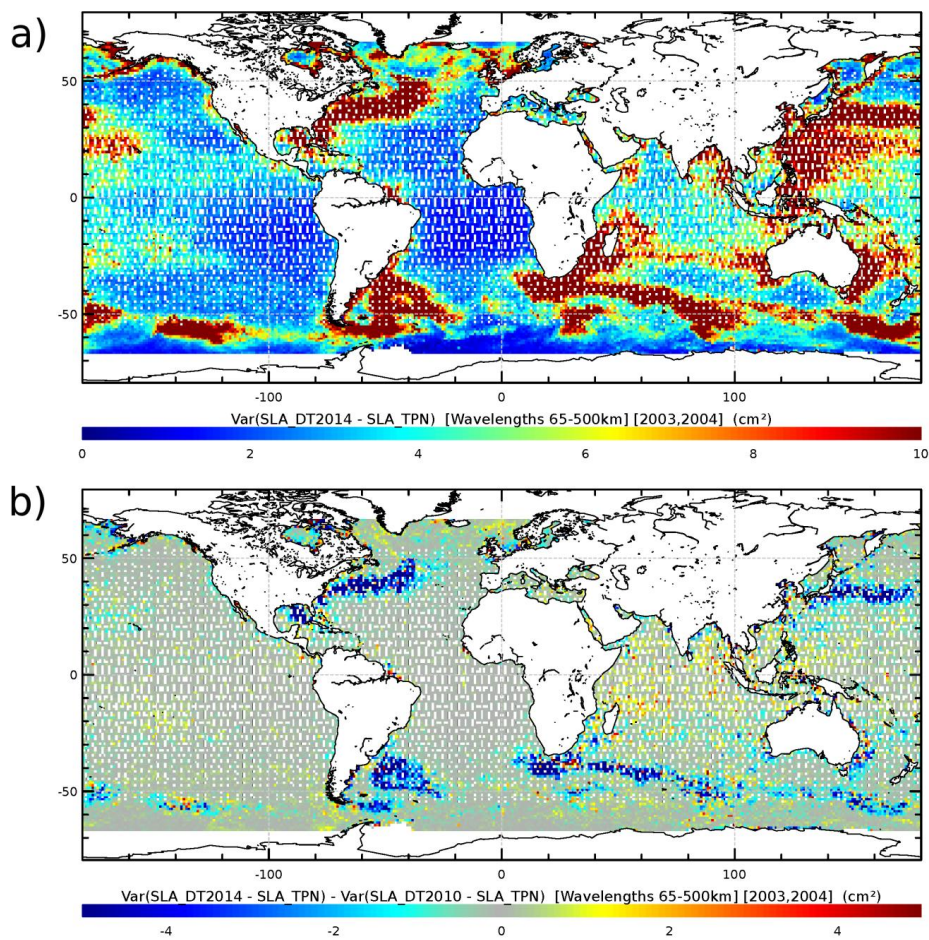
2

3 Figure 11: Evolution of the mean EKE over the global ocean, deduced from the DT2014

4 reprocessed product (black line) and the previous DT2010 version referenced on the 20-y

5 period (black dots lines) or on the 7-y period (grey dots lines).

6



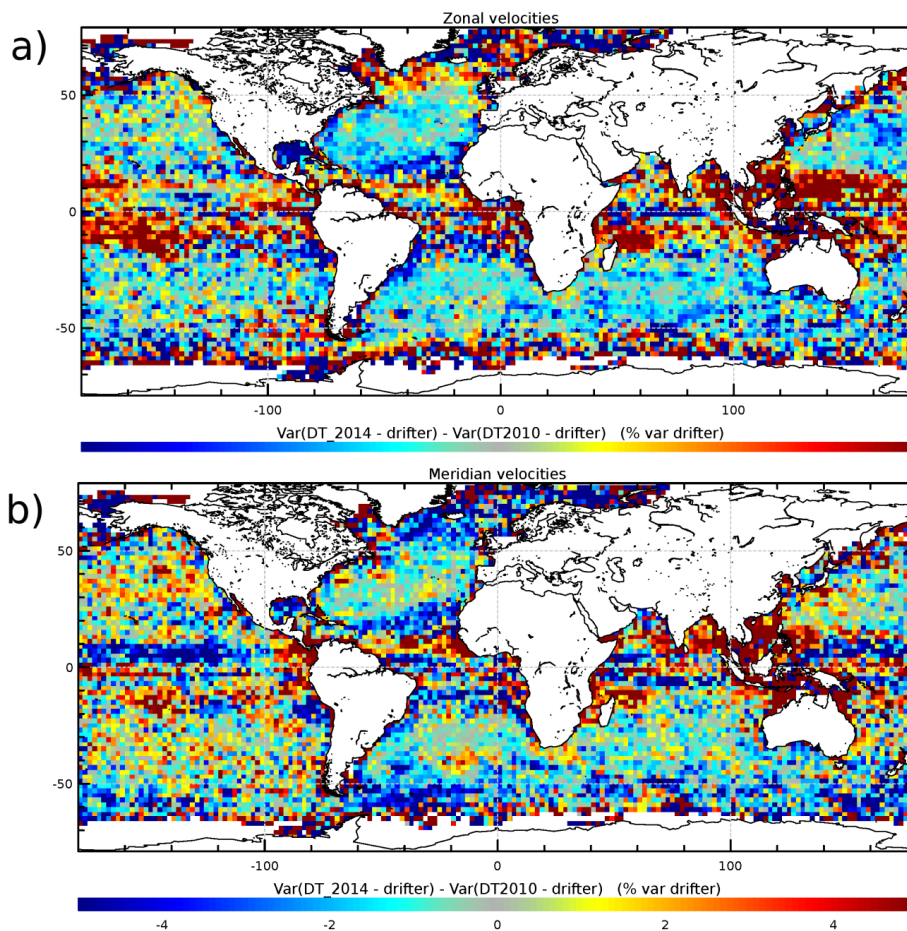
1

2 Figure 12: a) variance of the differences between gridded DT2014 two-sat-merged products  
 3 and independent TPN along-track measurements. b) variance reduction compared with the  
 4 results obtained with the DT2010 products. Statistics are presented for wavelength ranging  
 5 65-500 km. (unit =  $\text{cm}^2$ )

6



1



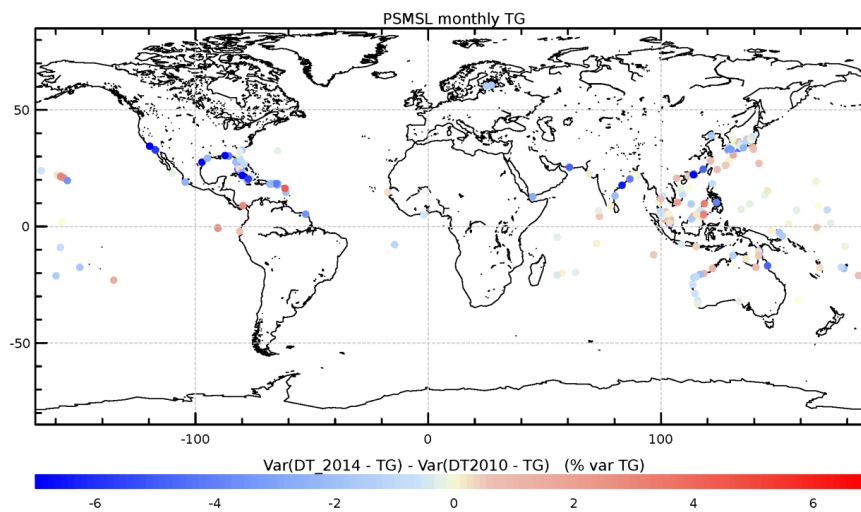
2

3 Figure 13: Variance reduction of the geostrophic current differences between altimeter  
4 gridded products and drifters measurements, when using DT2014 rather than DT2010  
5 products. The variance reduction is expressed in % of the drifter variance. Zonal (a) and  
6 Meridian (b) component differences.

7



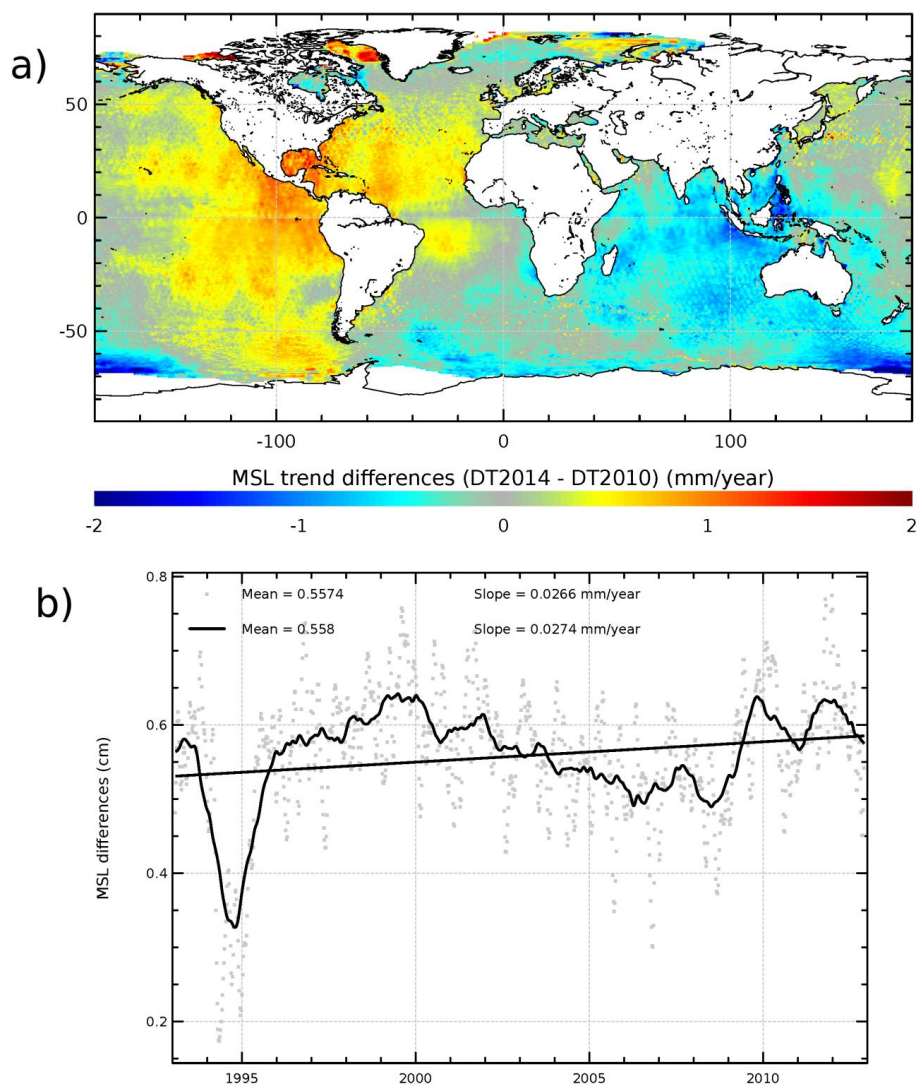
1



2

3 Figure 14: Variance reduction of the sea level differences between altimeter gridded products  
4 and tide gauges measurements, when using DT2014 rather than DT2010 products. Monthly  
5 TG from PSMSL.

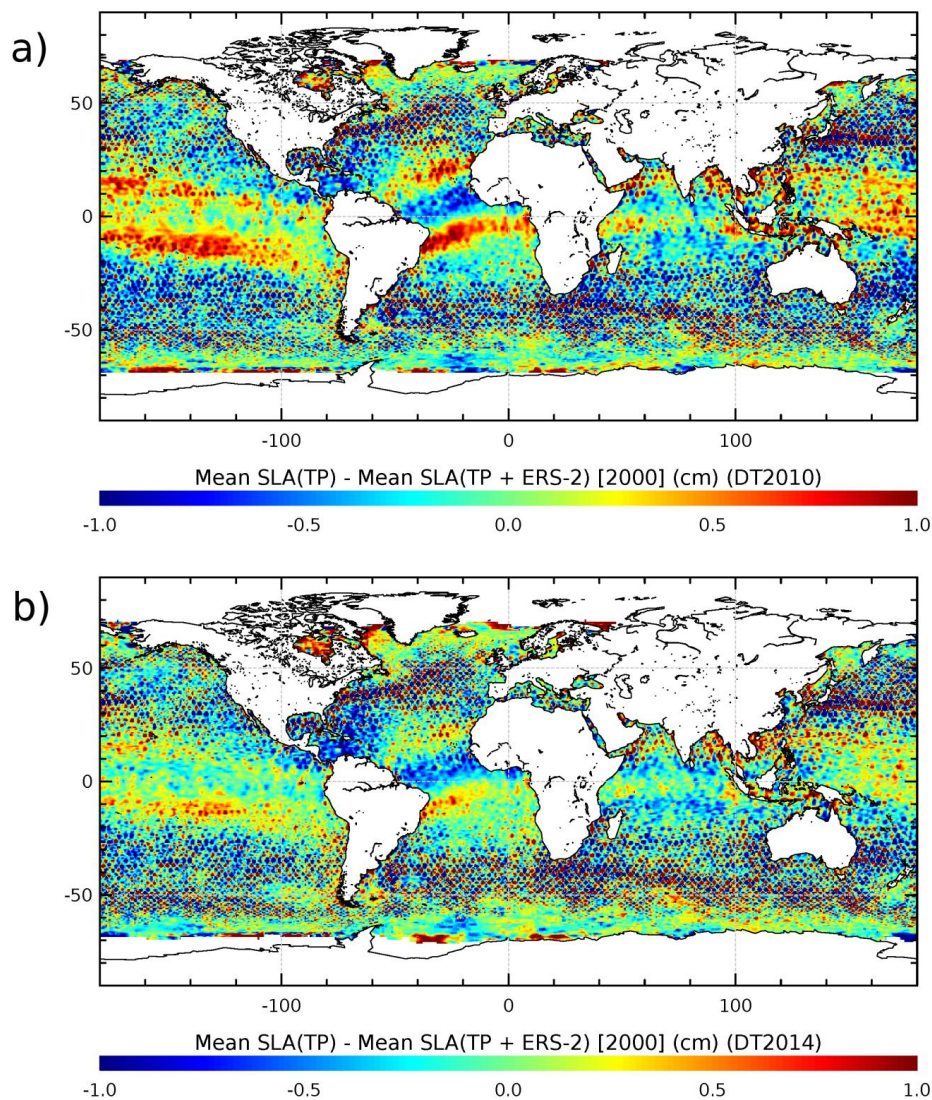
6



1

2 Figure 15: a) MSL trend differences between DT2014 and DT2010 products. MSL estimated  
3 over the [1993, 2012] period. b) MSL differences between DT2014 and DT2010.

4



1

2 Figure 16:: Difference of the mean SLA over the year 2000, measured with TP only, and with  
3 the merged TP+ERS-2 product. Comparison done for the DT2010 (a) and DT2014 (b)  
4 products.